CZECH TECHNICAL UNIVERSITY IN PRAGUE
FACULTY OF MECHANICAL ENGINEERING

DEPARTMENT OF FLUIDS DYNAMICS
AND THERMODYNAMICS

Prediction of thermodynamic properties of gas mixtures using the Peng-Robinson equation of state

Thesis supervisor: Doc. Ing. Václav Vacek, CSc.

June, 2015

Michal Haubner

Prohlášení

Prohlašuji, že jsem tuto bakalářskou práci vypracoval samostatně pod vedením vedoucího práce Doc. Ing. Václava Vacka, CSc., na Ústavu fyziky Fakulty strojní ČVUT v Praze a na zařízení, které bylo realizováno z grantových prostředků ústavu. Při vypracování jsem použil pouze podklady uvedené v seznamu na konci této práce.

Nemám závažný důvod proti užití tohoto školního díla ve smyslu § 60 zákona č. 121/2000 Sb., o právu autorském, o právech souvisejících s právem autorským a o změně některých zákonů (autorský zákon), pokud tak bude učiněno po dohodě s vedoucím práce a Ústavem fyziky Fakulty strojní ČVUT.

V Praze dne: ....

Michal Haubner

Acknowledgements

I wish to express gratitude to my thesis supervisor Doc. Ing. Václav Vacek, CSc. for sharing his professional outlook and insightful guidance throughout this interesting field of science.

Also, I would like to thank my family and friends for supporting me in every way possible during the course of my studies.

ČESKÉ VYSOKÉ UČENÍ TECHNICKÉ V PRAZE
Fakulta strojní, Ústav mechaniky tekutin a termodynamiky
Technická 4, 166 07 Praha 6 Akademický rok: 2014/2015

ZADÁNÍ BAKALÁŘSKÉ PRÁCE

pro: **p. Michala HAUBNERA**

program: **Teoretický základ strojního inženýrství**

obor: **bez oboru**

název česky: **Výpočet termodynamických vlastností směsí plynů užitím Pengovy a Robinsonovy stavové rovnice**

název anglicky: **Prediction of thermodynamic properties of gas mixtures using the Peng-Robinson equation of state**

Zásady pro vypracování:

1) Vypracujte rešerši na dané téma.

2) V Matlabu naprogramujte Jobackovu příspěvkovou metodu pro odhad termodynamických vlastností látek.

3) Použijte jednoduchá směšovací pravidla umožňující určení termodynamických vlastností směsí.

4) Pomocí derivací Pengovy a Robinsonovy stavové rovnice sestavte rovnici pro výpočet rychlosti zvuku ve směsi plynů a porovnejte výpočty s experimentálními daty rychlosti zvuku ve směsi chladiv C_3F_8 a C_2F_6.

Rozsah průvodní zprávy: 30 - 40

Rozsah grafických prací: grafy, schémata

Seznam doporučené literatury:

1) Nožička, J.: Základy termomechaniky. Nakladatelství ČVUT 2004, ISBN 80-01-02409-1
2) Novák J., et al. Termodynamické vlastnosti plynů. 1st ed. Praha: VŠCHT Praha, 2007, ISBN 978-80-7080-003-4.
3) Peng D.Y., Robinson D. B. A New Two-Constant Equation of State. Industrial & Engineering Chemistry Fundamentals. 1976. 15 (1), 59-64. DOI: 10.1021/i160057a011.
4) Poling B. E., Prausnitz J. M., and O´Connel J. P. The Properties of Gases and Liquids. New York: McGraw-Hill, 2001, ISBN: 0070116822.

Vedoucí bakalářské práce: Doc. Ing. Václav Vacek, CSc.

Konzultant bakalářské práce: Ing. Martin Doubek

Datum zadání bakalářské práce: 30. 04. 2015

Datum odevzdání bakalářské práce: 19. 06. 2015

Prof. Ing. Jiří Nožička, CSc.
Vedoucí Ú 12112

Prof. Ing. Michael Valášek, DrSc.
Děkan fakulty

V Praze dne 30. 4. 2015

Anotační list - Annotation

Author:	Michal Haubner
Téma:	Výpočet termodynamických vlastností směsí plynů užitím Pengovy a Robinsonovy stavové rovnice
Title:	Prediction of thermodynamic properties of gas mixtures using the Peng-Robinson equation of state
Academic year:	2014 – 2015
Field of study:	Thermodynamics
Department:	Faculty of Applied Physics
Thesis supervisor:	Doc. Ing. Václav Vacek, CSc.
Bibliographic data:	41 pages, 6 tables, 26 pictures
Klíčová slova:	Pengova a Robinsonova stavová rovnice, stavová rovnice, reálný plyn, příspěvková metoda, termodynamické vlastnosti, směšovací pravidla, chladiva, rychlost zvuku
Keywords:	Peng-Robinson equation of state, state equation, real gas, gas mixture, group contribution method, thermodynamic properties, mixing rules, refrigerants, speed of sound
Anotace:	Tato bakalářská práce shrnuje základní termodynamické poznatky potřebné pro výpočet rychlosti zvuku ve směsích reálných plynů užitím Pengovy a Robinsonovy stavové rovnice. Dále jsou užity dvě příspěvkové metody pro určení termodynamických vlastností chladiv C_2F_6 and C_3F_8. Analyticky výpočtená rychlost zvuku ve směsích plynů N_2 a C_3F_8 je porovnána s měřeními provedenými na sonarové trubici. Nakonec je zhodnocena přesnost měření, zdroje chyb a celkový potenciál těchto metod.
Abstract:	This bachelor thesis summarizes basic thermodynamic concepts necessary for calculation of speed of sound in mixtures of real gases using the Peng Robinson equation of state. Moreover, two different group contribution methods are used to estimate thermodynamic properties of refrigerants C_2F_6 and C_3F_8. The analytical prediction of speed of sound in mixtures of N_2 and C_3F_8 is then confronted with experimental data measured on sunar tube gas analyzer. Finally, the accuracy, sources of error and overall potential of this approach is discussed.

Contents

1 Introduction 1
2 Thermodynamic properties of fluids 2
2.1 Introduction 2
2.2 Main thermodynamic properties of fluids 2
2.2.1 Critical point 2
2.2.2 Reduced state variables 3
2.2.3 Acentric factor 3
2.2.4 Heat capacity 4
2.2.5 Poisson's ratio 5
2.3 Speed of sound 5
2.3.1 Sound wave propagation 5
2.3.2 Speed of sound 6
3 Description of state behaviour 7
3.1 Introduction 7
3.2 Ideal gas 7
3.3 Compressibility factor 8
3.4 Real gases 9
3.5 Equations of state 9
3.6 Van der Waals 10
3.7 Redlich - Kwong 11
3.8 Peng - Robinson 12
3.9 Accuracy of Redlich-Kwong and Peng-Robinson EOS 13
4 Application for mixtures 15
4.1 Introduction 15
4.2 Ideal mixture of real gases: Kay's Rule 15
4.3 Real mixture of real gases: Interaction coefficients 16
5 Speed of sound in a mixture using Peng-Robinson EOS 17
5.1 Outline 17
5.2 Equation of state derivatives 17
5.3 Peng Robinson EOS for mixtures 18
6 Group contribution methods 19
6.1 Introduction 19
6.2 Basic methods 20
6.3 Group decomposition 20
6.4 Method of Joback and Reid 21
6.4.1 Application of Joback and Reid method 21
6.5 Method of Constantinou and Gani 22
6.5.1 Application of Constantinou and Gani method 22

6.6 Accuracy of methods compared to NIST database 23
6.7 Literature research conclusion 23
7 MATLAB implementation 24
7.1 Group contribution methods 24
7.2 Mixture parameters for Peng-Robinson equation 24
7.3 Speed of sound calculation 25
8 Measurement 26
8.1 Introduction 26
8.2 Experiment setup 26
8.2.1 Principle 26
8.2.2 Construction 27
8.3 Data acquisition 27
8.4 Measurement procedure 29
8.4.1 Emptying the sonar tube 29
8.4.2 Defining a mixture 29
8.4.3 Creating a mixture 29
8.4.4 Measurement of an isochore 30
8.4.5 Measurements at different isochores 31
8.5 Data processing 32
8.5.1 Outline 32
8.5.2 Data processing 32
9 Theory and measurement comparison 33
9.1 Outline 33
9.2 Mixtures of N_2 with C_3F_8 33
9.3 Mixture 1 (95% N_2 and 5% C_3F_8) 34
9.4 Mixture 2 (6% N_2 and 94% C_3F_8) 35
9.5 Mixture 3 (16% N_2 and 84% C_3F_8) 36
9.6 Summary of experimental investigation 37
10 Summary and conclusions 39
10.1 Findings of the theoretical part 39
10.2 Results of the measurement 39
10.3 My own contribution 40
10.4 Conclusion 40
10.5 Suggestion for further study 41
11 Bibliography 42
12 List of figures 44
13 List of tables 45
14 Appendix A – Developed MATLAB code 45
14 Appendix B – Enclosed CD 53

Nomenclature

Latin letters

a	Parameter in equations of state	[Pa.m^6.mol^{-2}]
b	Parameter in equations of state	[m^3.mol^{-1}]
c	Speed of sound	[m.s^{-1}]
$C_{p,V}$	Molar heat capacity at constant pressure, volume	[J.mol^{-1}.K^{-1}]
h	Specific enthalpy	[J.kg^{-1}]
n	Amount of moles	[mol]
p	Pressure	[Pa]
p*	Reduced pressure	[-]
R	Universal gas constant	[J.mol^{-1}.K^{-1}]
T	Temperature	[K]
T*	Reduced temperature	[-]
u	Specific internal energy	[J.kg^{-1}]
V	Volume	[m^3]
V*	Reduced volume	[-]
x	Molar fraction	[-]

Greek letters

κ	Poisson's ratio	[-]
ω	Acentric factor	[-]

Superscripts

o	Ideal gas property
R	Residual value to an ideal gas property
*	Reduced variable

Subscripts

C	Critical value
m	Molar

Abbreviations

IG	Ideal Gas
RG	Real Gas
EOS	Equation of State
SOS	Speed of Sound
VdW	van der Waals
PR	Peng – Robinson
RK	Redlich – Kwong
JR	Joback – Reid
CG	Constantinou – Gani

1 Introduction

Thermodynamics similarly to other sciences attempts to create universally applicable theories, which can be used to solve variety of problems with just a small set of equations. It is essential for all engineering applications to understand thermodynamic properties of a continuum. However, the difficulty of this task becomes apparent as there are more than 100 elements in the periodic table. Each of them has specific chemistry and they all together create millions of compounds and even more possible mixtures. The motivation for describing a continuum escalated quickly during the industrial revolution with a strong need of grasping the water vapour to power steam engines (and turbines later on). Then it even intensified with an onset of petroleum industry, combustion engines, but also chemistry, medicine, food processing industry, etc. All these fields have one need in similar, to describe and predict compound's ability to store or transfer energy, change phase, or react with each other, all this taking place under various conditions.

This thesis is motivated by direct application of the presented phenomena to in-situ measurement of gas composition using sonar tube gas analyser. Given the fact that the sound-wave propagation through a medium depends greatly on its properties, the sound speed is a good indicator of medium's composition, temperature and pressure. Also, the speed of sound measurement essentially consists of distance and time measurement, both of which can be performed very easily and accurately, resulting in precise knowledge of speed of sound and composition, respectively.

In the introductory part a brief review of the most important concepts of thermodynamics is put forward. It begins with description of ideal and real gas behaviour, introducing critical point and reduced state variables and is followed by thermodynamic properties, such as heat capacities, speed of sound and compressibility factor.

Further, various equations of state describing a real gas are presented and their accuracy and field of use is discussed. Subsequently, placing a particular interest on the Peng-Robinson's equation, its application is extended for mixtures and its derivatives are used to calculate the speed of sound in a mixture of real gases.

In addition, two group contribution methods for estimating thermodynamic properties of organic compounds (Joback-Reid, Constantinou-Gani) are presented and their accuracy and applicability is discussed and compared to the table values (NIST). The emphasis is placed on compounds of engineering interest, such as those used as refrigerants and working fluids in thermodynamic systems.

Finally, the theoretical prediction of speed of sound is confronted with measurements taken on sonar tube gas analyser experiment which was developed earlier at the Faculty of Applied Physics at CTU Prague.

Furthermore, both the analytical and experimental part of this thesis was implemented into MATLAB. Therefore, the group contribution methods, Peng-Robinson equation of state and speed of sound in mixtures can be easily evaluated, once a user defines composition of a mixture and a pressure and temperature range.

2 Thermodynamic properties of fluids

2.1 Introduction

Apart from the intuitive variables like pressure p, temperature T and volume V, many different and more abstract properties have been derived over time, each describing a medium in a manner that facilitates certain calculations and that has a very concrete meaning in certain processes. Amongst these is internal energy U, enthalpy H, entropy S, heat capacities $C_{p,V}$, speed of sound c, etc.

2.2 Main thermodynamic properties of fluids

For all elements and their compounds, there is a unique phase diagram and yet, all these diagrams are alike and have certain points and regions where different substances behave in the same manner. The critical point (Fig. 1.) to which we relate (reduce) properties of different fluids is of greatest importance.

2.2.1 Critical point

The critical point is located at the end of vapour-liquid phase equilibrium curve, past which there is no phase boundary, the difference between liquid and its gaseous phase vanishes and the gas approaches the ideal gas (IG) behaviour (the particle's kinetic energy prevails upon the attractive forces). Hereafter, we will primarily focus

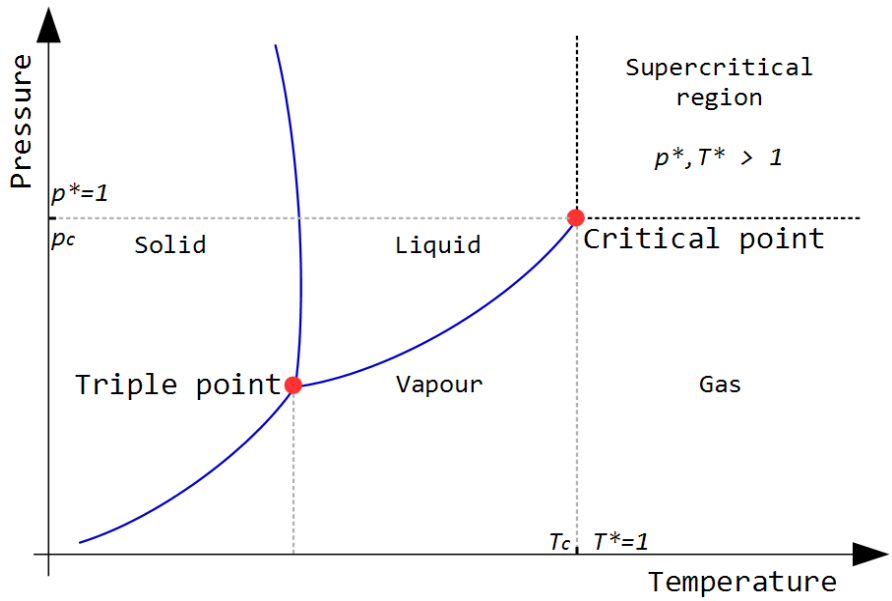

Fig. 1: p-T projection of a phase diagram (simplified). The critical and triple points are marked in red, connected by the liquid-vapour line in blue. Note the supercritical region and corresponding values of reduced pressure and temperature

on the subcritical (liquid, vapour and gas) region of the phase diagram. The critical point is defined by the critical values of temperature T_c [K], pressure p_c [Pa] and molar volume $V_{m,c}$ [m^3.mol^{-1}] (or molar density ρ_c, which is inverse volume). The precise knowledge of the critical point's position in the phase diagram is essential to the vast majority of state equations, theory of corresponding states and different techniques used in thermodynamics.

2.2.2 Reduced state variables

According to the theorem of corresponding states (formulated by Van der Waals), all real gases behave in a similar way when compared in terms of their dimensionless state variables, i.e. state variables reduced by their values at the critical point. Thus we define the reduced pressure p^* [-], temperature T^* [-], volume V^* [-] and density ρ^* [-].

$$p^* = \frac{p}{p_c} \qquad T^* = \frac{T}{T_c} \qquad V^* = \frac{V}{V_c} \qquad \rho^* = \frac{\rho}{\rho_c} \qquad [1] \qquad 2.1$$

2.2.3 Acentric factor

So called acentric factor ω [-], proposed by K. Pitzer in 1955, was introduced as a corrective parameter in the theory of corresponding states. Despite its rigorous derivation using vapour pressure (2.2*)*, the acentric factor essentially characterises deviation of a molecule from an ideal sphere (Fig. 2). Nowadays, it is the fourth important characteristic of a fluid (after the p_C, V_C, T_C values at the critical point) and is involved in majority of theories describing state behaviour. According to [2, p. 29], or [4, p. 3], the acentric factor ω is defined in terms of saturation pressure and critical pressure at reduced temperature of $T^*=0.7$.

$$\omega = -\log_{10}\frac{p^s_{0.7}}{p_c} - 1 \qquad [-] \qquad 2.2$$

Its value approaches *0* for gases comprised of spherical molecules (noble gases, except He), it can have negative values (H, He), but generally its values are greater than *0*. The less symmetric the molecule is, the larger the ω. See Table 1. and note the heavy straight chain n-Hectane $C_{100}H_{202}$ with $\omega=2.4$.

Table 1.: Acentric factors for various chemicals. Data is retrieved from NIST REFPROP software [6], and from Yaws, C. L.: Thermophysical Properties of Chemicals and Hydrocarbons [15].

Compound	Acentric factor ω [-]	
	NIST	Yaws
He	-0.385	-0.385
H_2	-0.219	-
O_2	0.0222	0.0222
N_2	0.0372	0.0377
C_2F_6	0.2566	0.249
C_3F_8	0.3172	0.327
H_2O	0.3443	0.3449
$C_{100}H_{202}$	-	2.436

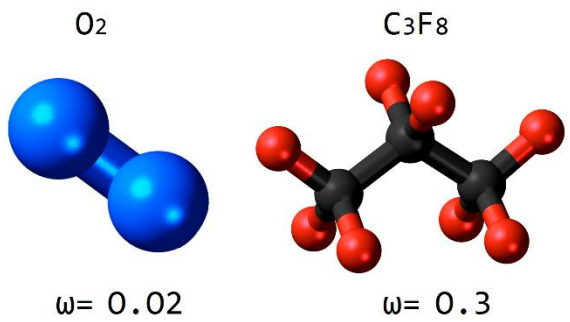

Fig. 2.: Acentric factor. The more symmetric the molecule is, the lesser acentric factor.

2.2.4 Heat capacity

The concept of heat capacity arises immediately while imposing heat on a fluid. Generally, it can be done either at constant pressure, constant volume or neither of these. Yet the constant pressure or volume cases have preeminent meaning in the real-life applications. According to [5] specific heat capacities $c_{p,v}$ [J.kg^{-1}.K^{-1}] can be calculated as the increase of specific enthalpy h [J.kg^{-1}] and specific internal energy U [J.kg^{-1}] divided by an increase of temperature T at constant pressure and constant volume, respectively.

$$c_p = \left(\frac{\partial h}{\partial T}\right)_p \qquad c_V = \left(\frac{\partial u}{\partial T}\right)_V \qquad [\,\mathrm{J.kg^{-1}.K^{-1}}] \qquad 2.3$$

Heat capacities can also be expressed with respect to the molar volume rather than mass, because this notion is more practical when dealing with gases.

$$C_p \qquad C_V \qquad [\,\mathrm{J}.mol^{-1}.\mathrm{K}^{-1}] \qquad 2.4$$

Thermodynamic properties of real substances are usually expressed as a sum of two terms. The first term (with *o* superscript) is representing the *ideal* behaviour, whereas the second term, called *residual* (R) is taking into account the non-ideal behaviour. This also applies to the heat capacities, which are in turn a sum of an ideal gas value and a residual value.

$$C_{p,V} = {C_{p,V}}^{o} + {C_{p,V}}^{R} \qquad [\,\mathrm{J.mol^{-1}.K^{-1}}] \qquad 2.5$$

The ideal heat capacities ${C_{p,V}}^{o}$ vary with temperature and are usually described in a form of polynomial, with the coefficients being either tabulated [21], or calculated knowing molecular structure (e.g. using group contribution methods, which will be described further on). Different authors tabulate N-degree polynomial coefficients a_i of either ${C_p}^{o}$, or ${C_V}^{o}$.

$${C_p}^{o}(T) = \sum_{i=0}^{N} a_i\, T^i \qquad [\,\mathrm{J.mol^{-1}.K^{-1}}] \qquad 2.6$$

To calculate the residual value of ${C_p}^{R}$, we can derive the residual internal energy U^R with respect to the temperature T (The symbols will be defined in following chapters).

$${C_V}^{R}(T) = \left(\frac{\partial U^R}{\partial T}\right)_V \qquad [\,\mathrm{J.mol^{-1}.K^{-1}}] \qquad 2.7$$

$${C_V}^{R}(T) = \frac{T.a''(T)}{\sqrt{8}\,b}\,\ln\left[\frac{Z + B(1+\sqrt{2})}{Z + B(1-\sqrt{2})}\right] \qquad [\,\mathrm{J.mol^{-1}.K^{-1}}] \qquad 2.8$$

Furthermore, the thermodynamic laws imply that for a real gas, the difference between $C_{p\,m}$ and $C_{V\,m}$ is generally a function of state variables [4, p. 164].

$$C_p - C_V = T\left(\frac{\partial V}{\partial T}\right)_P \left(\frac{\partial P}{\partial T}\right)_V \qquad [\,\mathrm{J.mol^{-1}.K^{-1}}] \qquad 2.9$$

If accounting for the ideal gas behaviour only and leaving out the residual term, this relation further simplifies, so that the difference between C_p and C_V is equal to the universal gas constant R.

$$C_p{}^o - C_V{}^o = R = 8.3144621 \qquad [\,\mathrm{J.mol^{-1}.K^{-1}}] \qquad 2.10$$

Given the relations above, we can now write equations for both real heat capacities.

$$C_V(T) = \sum_{i=0}^{N} a_i\, T^i + C_V{}^R(T) - R \qquad [\,\mathrm{J.mol^{-1}.K^{-1}}] \qquad 2.11$$

$$C_p(T) = \sum_{i=0}^{N} a_i\, T^i + C_V{}^R(T) - R + T\left(\frac{\partial V}{\partial T}\right)_P \left(\frac{\partial P}{\partial T}\right)_V \qquad [\,\mathrm{J.mol^{-1}.K^{-1}}] \qquad 2.12$$

2.2.5 Poisson's ratio

At last, the ratio between the two heat capacities is defined and called the Poisson ratio κ [-]. This ratio has an immediate and important application in adiabatic processes, i.e. where no heat is exchanged between a system and its surroundings. For instance, an adiabatic expansion and compression, which essentially is a sound wave propagation.

$$\frac{C_p}{C_V} = \kappa \qquad [-] \qquad 2.13$$

2.3 Speed of sound

2.3.1 Sound wave propagation

In a fluid continuum (liquid, vapour, gas), the sound wave propagates predominantly through compression waves (also called longitudinal), which means, that the displacement of molecules has the same direction as the wave propagation (Fig. 3). Other types of waves (transverse waves) are not present, because ideal liquids cannot support shear strain, which would enable other types of wave propagation.

In an ideal case, an excitation causes particles to oscillate around an equilibrium position and the movement of particles spreads in a direction perpendicular to the pressure gradient. The rate at which this movement spreads is called the speed of sound and is dependent mainly on composition, temperature and pressure of the concerned gas. Because this process usually happens faster than any heat can be dissipated, it can be considered isentropic.

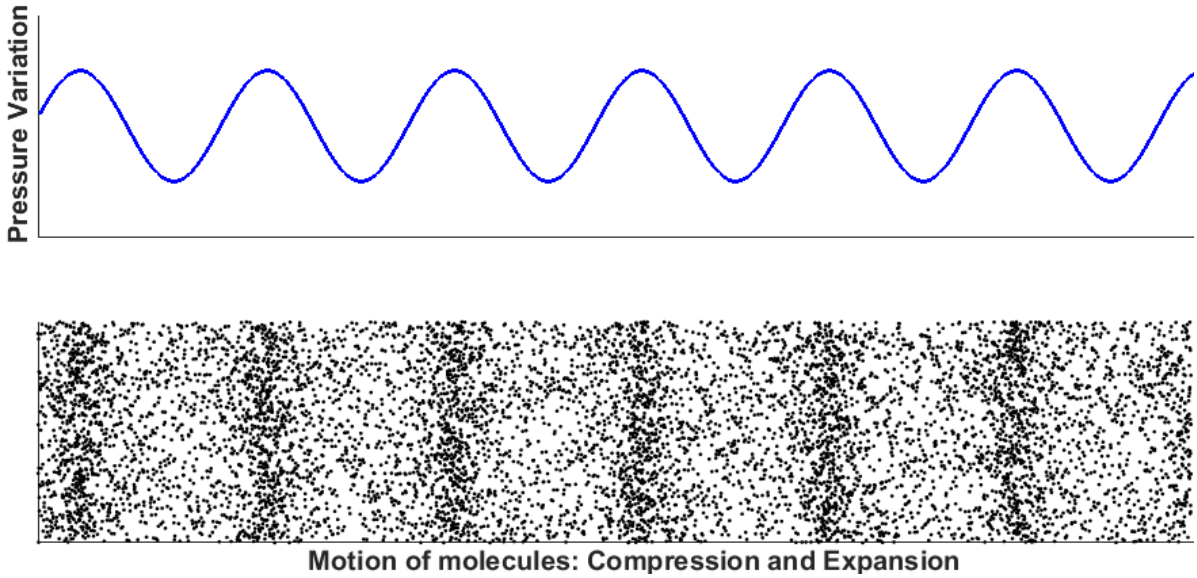

Fig. 3.: Sound wave propagation. Compression and expansion of gas molecules results in a pressure variation, which propagates across a fluid.

2.3.2 Speed of sound

Speed of sound (hereafter abbreviated as SOS) in a medium is an important property. Firstly, because it is directly measurable and secondly, it serves well as an indicator of medium properties, in the means of temperature, pressure and composition. While applying some reasonable hypotheses of unidirectional, non-dispersive and adiabatic (isentropic) sound wave propagation, it can be derived that the SOS in a real gas has the following form.

$$c = \sqrt{\left(\frac{\partial p}{\partial \rho}\right)_S} \qquad [\,\mathrm{m}.s^{-1}] \qquad 2.14$$

The isentropic derivative can be broken down into a form, where the derivative is evaluated from an equation of state. The parameter M [g/mol] is the molar mass of a gas, or an apparent molar mass of a mixture of gases.

$$c = V_m \sqrt{\kappa \frac{1}{M}\left(\frac{\partial p}{\partial V}\right)_T} \qquad [\,\mathrm{m}.s^{-1}] \qquad 2.15$$

In case of an ideal gas, the equation for speed of sound c can be further simplified into the following form.

$$c^o = \sqrt{\frac{{C_p}^o}{{C_V}^o}\frac{R\,T}{M}} \qquad [\,\mathrm{m}.s^{-1}] \qquad 2.16$$

These equations are applicable to mixtures as well, provided that proper mixing rules are used [7].

3 Description of state behaviour

3.1 Introduction

Based upon the previous knowledge of Gay-Lussac's, Boyle's and Dalton's law, which are essentially special cases of ideal gas behaviour, the ideal gas concept was formulated by Clapeyron in the 18th century. However, major drawbacks, including absolute compressibility, lack of phase transitions and prediction inaccuracies were a subject of concern to the scientists and engineers of the epoch.

3.2 Ideal gas

As mentioned in [1], the IG state equation was formulated as follows. The p is the pressure [Pa], V is volume [m^3], T is temperature [K], n is number of moles [mol] and R [J.mol^{-1}.K^{-1}] is the universal gas constant.

$$p\,V = n\,R\,T \qquad [J.mol^{-1}] \qquad 3.1$$

Dividing the equation by n and defining the molar volume $V_m = V/n$ [m^3.mol^{-1}], we obtain a form referring to a unitary amount (n = 1 mol) of gas. This molar volume will be used in the equations further on.

$$p\,V_m = R\,T \qquad [J.mol^{-1}] \qquad 3.2$$

The universal gas constant R is defined as a product of Avogadro's constant N_A and Boltzmann's constant k_B.

$$R = N_A\,.\,k_B = 6.0221418\,.\,10^{23} mol^{-1}.\,1.3806488\,.\,10^{-23} J.K^{-1} \qquad 3.3$$

$$R = 8.314462 \qquad [J.K^{-1}.mol^{-1}] \qquad 3.4$$

The IG EOS was derived under a number of hypotheses: absolute compressibility, constant molar volume (independence of gas composition) and intermolecular forces being negligible behind particles' kinetic energy. These assumptions are only plausible in a very restricted region of states, such as high temperatures and low pressures. This led to further improvements.

3.3 Compressibility factor

It became apparent almost immediately that real gases do not completely conform to the ideal gas description and that these deviations from the ideal behaviour have to be described.

As a result, a ratio between the real gas volume and an ideal gas volume (at a specified state point) is defined and referred to as the *compressibility factor Z* [1]. By definition the compressibility of an ideal gas $Z^o=1$, whereas the compressibility Z of real gases reaches values from *0* to about *2*. We can write the following relation.

$$Z = \frac{V_m}{V_m{}^o} = \frac{p\,.\,V_m(p,T)}{R\,.\,T} \qquad [1] \qquad 3.5$$

The dependence of $V_m(p,T)$ can be expressed from one of the state equations. Thus the equation eventually becomes a specific notation of any EOS. Moreover, it is favourable to employ the dimensionless state variables of temperature T^* and pressure p^*. In Fig. 4. we see approximately the same behaviour regardless of the fluid concerned, which is a result of the principle of corresponding states.

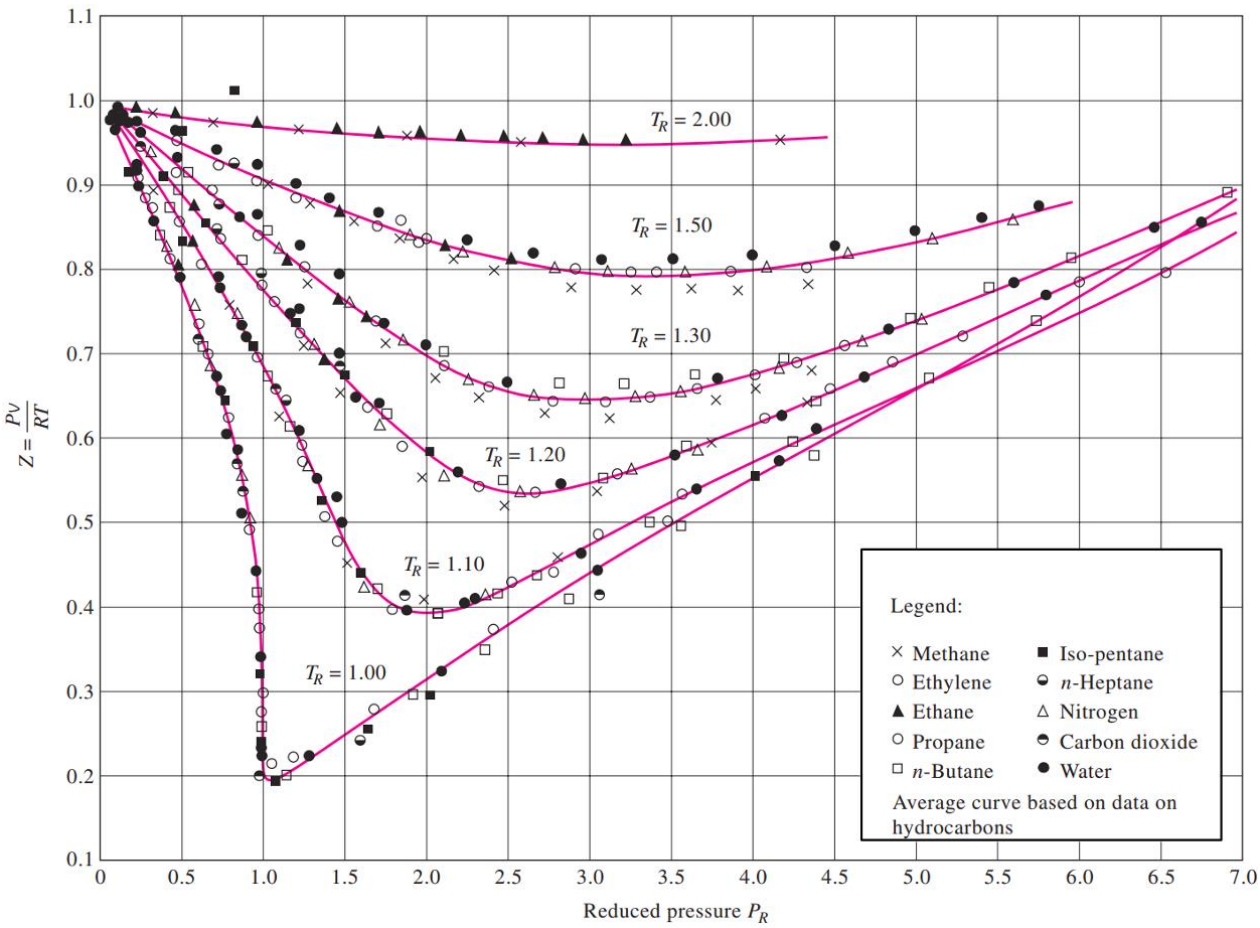

Fig. 4.: Generalized compressibility chart. Note the isotherms and the similar behaviour of various substances. Image source: [20].

The remaining variance between the experimental and predicted values of Z was the reason to employ the acentric factor ω [-] as the 4th fluid characterising parameter.

In the end, the compressibility factor is obtained as a function of reduced state variables and acentric factor.

$$Z = f(p^*, V^*, T^*, \omega) \qquad [1] \qquad 3.6$$

However, it is convenient to keep T^* constant in the calculation to obtain isotherms in the compressibility chart [9, p.112].

$$Z = f(p^*)_{T^*=const.} \qquad [1] \qquad 3.7$$

3.4 Real gases

Not long after the ideal gas theory was published, the first attempt was made to correct the above-mentioned deficiencies. By the end of the 20th century, numerous different equations of state (EOS) were developed, each of which is usually meant to meet the needs of a specific domain of application. Generally, the accuracy of these equations rises along with the equations' complexity and number of parameters needed to perform the calculation.

3.5 Equations of state

The physical reality of the phase diagram has some implications, that a convenient EOS should meet [2, p. 11]. At the critical point the 1st and 2nd partial derivatives with respect to volume need to be zero and the 3rd one is negative.

$$\left(\frac{\partial p}{\partial V}\right)_C = 0 \qquad \left(\frac{\partial^2 p}{\partial V^2}\right)_C = 0 \qquad \left(\frac{\partial^3 p}{\partial V^3}\right)_C < 0 \qquad 3.8$$

These conditions on partial derivatives, applied at the critical point, lead immediately to the conclusion that at least a cubic polynomial (in volume) is needed to describe the real gas behaviour in the region of p-T diagram under the critical point. The presence of the 3rd order polynomial in the equation enables the description of liquid phase and the region of wet steam under the critical point (Fig. 5). This fact has given rise to a large group of so-called cubic equations of state.

Nevertheless, the liquid-vapour region of the phase diagram remains problematic, because it does not arise directly from cubic equations of state. It has to be added artificially to properly reflect the physical reality of the phenomena. This is done in Fig. 5, where a subcritical isotherm(red) is substituted by a straight line *L-V* (blue). This line is positioned so that the integral of the of the isotherm curve beneath *L-I* is equal to that above *I-V* line. The whole saturation curve is then determined by following this procedure for different subcritical isotherms.

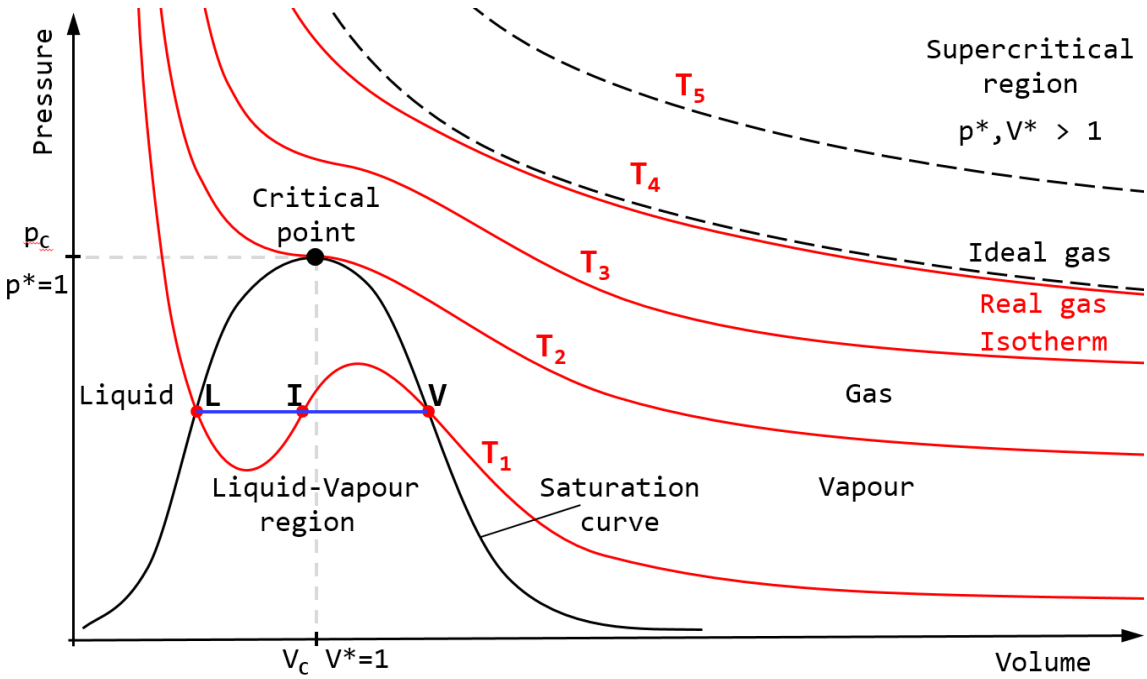

Fig. 5.: Schematic p-V diagram of a real gas. Note the difference in behaviour of a liquid in the two regions below and above critical point.

To be correct, the isotherm, which is predicted by a state equation in between the *V-I* points, can be reached (part of it) in a form of supersaturated vapour, i.e. vapour which has been cooled below the dew point, but condensation has not occurred yet. The same principle applies for the *L-I* part of the isotherm, which corresponds to superheated liquid, i.e. liquid, which was heated above its boiling point, but the boiling process did not yet begin. However, both these states are metastable, thus are not of our interest.

Concerning the supercritical region (above the critical point), the state equations are directly applicable here. For higher temperatures and low pressures, a real gas tends to behave more like an ideally. So should any EOS approach the IG EOS in the supercritical region of the p-V diagram.

3.6 Van der Waals

The first successful attempt to extend the validity of ideal gas equation is a result of a qualitative approach of Van der Waals, who formulated the historically first cubic EOS. As mentioned in [3] and [1], Van der Waals assumed that pressure in a fluid is a sum of attractive and repulsive pressure terms. (This concept was later re-derived using the Lennard-Jones potential of attractive and repulsive intermolecular forces.)

$$p = p_A + p_R \qquad [Pa] \qquad 3.9$$

The attraction term accounts for intermolecular forces which come into effect for example on the system's boundary, where the particles are attracted back inside

the fluid, thus diminishing the gauge pressure (pressure measured by any kind of a manometer). Whereas the repulsion pressure term takes into account proper volume of molecules, which needs to be subtracted from the molar volume in order to get the real volume accessible to the particles' motion.

$$p_A = -\frac{a}{{V_m}^2} \qquad [Pa] \qquad 3.10$$

$$p_R = \frac{R\,T}{V_m - b} \qquad [Pa] \qquad 3.11$$

The two terms sum up into the Van der Waals equation of state. It can be arranged in different forms [1, p. 65], either in terms of attractive and repulsive pressure, or in terms of molar energy. This second form is particularly explicative, because it can be easily compared to the IG EOS, and the corrections for attractive pressure and proper volume of molecules are clearly distinguishable.

$$p = \frac{R\,T}{V_m - b} - \frac{a}{{V_m}^2} \qquad [Pa] \qquad 3.12$$

$$\left(p + \frac{a}{{V_m}^2}\right)(V_m - b) = R\,T \qquad [J.mol^{-1}] \qquad 3.13$$

By applying the equation at the critical point, we obtain the coefficients a and b in terms of universal gas constant R, critical temperature T_c and critical pressure p_c. These critical quantities have to be known for a given substance and can either be found in the tables or calculated using some of the estimation methods mentioned further on.

$$a = \frac{27}{64}\frac{R^2\,{T_c}^2}{p_c} \qquad [Pa.m^6.mol^{-2}] \qquad 3.14$$

$$b = \frac{1}{8}\frac{R\,T_c}{p_c} \qquad [m^3.mol^{-1}] \qquad 3.15$$

3.7 Redlich - Kwong

In 1948 Redlich and Kwong (RK) put forward a two-constant cubic EOS. In [2] it is claimed to be the most accurate two *constant* EOS so far. Yet, this accuracy is conditioned by small molar mass of a gas (as it is shown later). Nonetheless, the pressure p is a sum of attractive and repulsive terms. The first term being the same as in VdW EOS, whereas the second term is more complex.

$$p = \frac{R\,T}{V_m - b} - \frac{a}{\sqrt{T}\,V_m(V_m + b)} \qquad [Pa] \qquad 3.16$$

Using the critical point to match the constants a and b of this equation gives the relations for a and b parameters.

$$a = 0.4274802336 \frac{R^2 \, {T_c}^{2.5}}{p_c} \qquad [Pa.m^6.mol^{-2}] \qquad 3.17$$

$$b = 0.08664034995 \, \frac{R \, T_c}{p_c} \qquad [m^3.mol^{-1}] \qquad 3.18$$

3.8 Peng - Robinson

This widely used cubic EOS was presented in 1975 by D.Y. Peng and D. B. Robinson [3,4]. Once more, this two-parameter (technically one constant and one parameter) equation is formally similar to the VdW EOS. Yet, the a parameter in the attractive pressure term varies as a function of the temperature.

$$p = \frac{R \, T}{V_m - b} - \frac{\mathrm{a}(T)}{V_m(V_m + b) + b(V_m - b)} \qquad [Pa] \qquad 3.19$$

Again, by applying the equation at the critical point, we obtain the constant b in terms of the critical temperature T_c, critical pressure p_c and the universal gas constant R. Moreover, the parameter a is also dependent on the temperature T and on the acentric factor ω [-], as it is apparent from the following equations. The acentric factor should be lower than 0.49 in order to use the mentioned polynomial for m.

$$b = 0.0077796074 \, \frac{R \, T_c}{p_c} \qquad [m^3.mol^{-1}] \qquad 3.20$$

$$a = a_c \, . \, \alpha(T) \qquad [Pa.m^6.mol^{-2}] \qquad 3.21$$

$$a_c = 0.45723553 \, \frac{R^2 \, {T_c}^2}{p_c} \qquad [Pa.m^6.mol^{-2}] \qquad 3.22$$

$$\alpha = \left[1 + m \, . \left(1 - \sqrt{T/T_c}\right)\right]^2 \qquad [1] \qquad 3.23$$

$$m = 0.374646 + 1.54226 \, \omega - \, 0.26992 \, \omega^2 \qquad [1] \qquad 3.24$$

It is useful for certain calculations to express the EOS in the form of compressibility factor. PR EOS can be put into form of a 3rd degree polynomial, with the parameters α, β, γ dependent on temperature, pressure and composition.

$$f(Z) = Z^3 + \alpha \, Z^2 + \beta \, Z + \gamma = 0 \qquad [1] \qquad 3.25$$

$$\alpha = B - 1 \qquad 3.26$$

$$\beta = A - 2B - 3B^2 \qquad A = aP/(RT)^2$$

$$\gamma = B^3 + B^2 - AB \qquad B = bP/RT$$

3.9 Accuracy of Redlich-Kwong and Peng-Robinson EOS

The state equations mentioned above feature accuracies varying not only on a region of a phase diagram, but also on a described gas. Different papers present accuracies from 2% to 20%, depending on the experiments' *p-T* range and also on a dataset of chemicals used for evaluation. However, in case of avoiding extreme (both small and large) values of state variables and not taking into account any strongly associating fluids, we usually get deviation in order of percents.

Table 2. shows data retrieved from work of Riazi and Mansoori [16]. Here, the authors gathered experimental data from NIST (National Bureau of Standards, 1974-82) and TRC Thermodynamic Table (Texas A&M University, 1986). Data included experimental values of density of organic compounds measured for temperatures of 90 - 1000 K and pressures from 0.01 - 70 MPa. This dataset was then compared to values of density predicted by RK and PR EOS. The accuracy of both state equations is listed for different compounds in terms of average absolute deviation (Eq. 3.27).

Table 2.: RK and PR EOS accuracy for density prediction of light and heavy compounds. AAD: Average Absolute Deviation [%]. Source: [16].

Compound		Molar mass [g/mol]	Number of Data Points	AAD [%]	
				RK	PR
Light compounds					
Oxygen	O_2	32.00	120	1.1	4.0
Methane	CH_4	16.04	135	0.9	4.5
Ethane	C_2H_6	30.07	157	2.3	4.2
Ethylene	C_2H_4	28.05	90	2.4	4.5
Propane	C_3H_8	44.10	130	3.4	3.9
Butane	C_4H_{10}	58.12	115	5.0	3.4
i-Butane	C_4H_{10}	58.12	183	4.7	4.9
Hexane	C_6H_{14}	86.18	100	6.2	1.8
Cyclohexane	C_6H_{12}	84.16	140	5.4	3.7
Benzene	C_6H_6	78.11	110	5.4	1.6
Toluene	C_7H_8	92.14	110	7.8	1.6
Heptane	C_7H_{16}	100.21	100	7.8	1.9
Octane	C_8H_{18}	114.23	80	9.2	2.5
i-Octane	C_8H_{18}	114.23	70	6.9	3.2
Total			1640	4.9	3.3
Heavy compounds					
Nonane	C_9H_{20}	128.20	35	15.5	3.4
Undecane	$C_{11}H_{24}$	156.31	35	18.0	5.4
Tridecane	$C_{13}H_{28}$	184.36	30	20.3	7.9
Heptdecane	$C_{17}H_{36}$	240.47	30	27.3	16.0
Icosane	$C_{20}H_{42}$	282.55	20	29.5	18.2
Triacontane	$C_{30}H_{62}$	422.81	20	41.4	32.5
Tetracontane	$C_{40}H_{82}$	563.08	20	50.9	44.4
Total			190	29.0	18.3
Overall			1830	12.9	8.3

$$AAD\ [\%] = \sum_{i}^{N} \left| \frac{X_i^{measured} - X_i^{theoretical}}{X_i^{theoretical}} \right| .100\ \% \qquad [\%] \qquad 3.27$$

To better illustrate and compare the RK and PR EOS accuracy as a function of a chosen compound, Table 2. data were plotted in Fig. 6. The Redlich-Kwong equation has smaller deviation than the Peng-Robinson EOS for the light compounds, i.e. those of molar mass lesser than about 50 g/mol. On the other hand, for compounds heavier than 50 g/mol, the Peng-Robinson EOS takes over in accuracy and is by about 5 - 10% more accurate than the Redlich-Kwong EOS.

Seemingly, accuracy of both state equations have predictive ability dependent on molar mass. However, this characteristic can be explained by the fact that the RK is a *two-constant* equation and does not engage the acentric factor ω in the calculation (ω has significant importance for heavier compounds). Whereas the PR EOS is a *one-constant* and *one-parameter* equation (parameter dependent on T and ω), thus more complex and more accurate, as one would anticipate.

Justified by this varying accuracy, the Peng-Robinson EOS was chosen for further calculations involving C_2F_6 and C_3F_8, both having molar mass greater than 100 g/mol. For compounds heavier than about 150 g/mol, one should choose a better suited EOS, because both RK and PR EOS cease to be reliable.

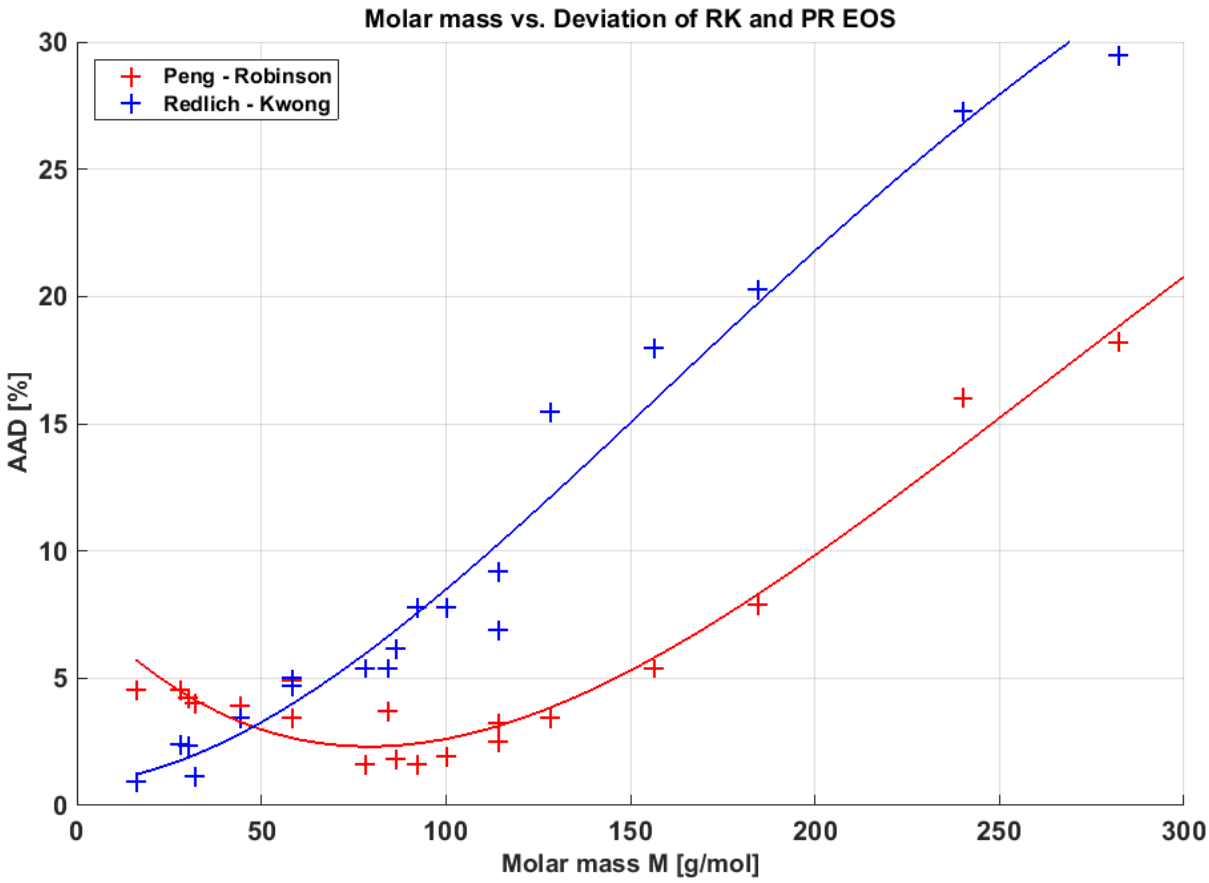

Fig. 6.: Accuracy of RK and PR EOS. Molar mass M [g/mol] of compounds vs. average absolute deviation AAD [%] of Redlich-Kwong and Peng-Robinson EOS prediction.

4 Application for mixtures

4.1 Introduction

The above-mentioned equations of state were derived assuming that we deal with a pure fluid. However, in technical practice, we often encounter mixtures of fluids, which need to be described as well. In order to use the existing equations of state for mixtures, their a and b parameters need to be calculated. It can be done in various ways, depending on an equation, desired accuracy or set of chemicals. The so-called 'mixing rules' usually take form of an arithmetic, geometric or other, more general type of average. Again, with an increasing accuracy the calculations become more complex.

4.2 Ideal mixture of real gases: Kay's Rule

The simplest mixing rule for an ideal mixture of real gases emerges quite naturally as a weighted average of pure components' properties [2, p. 34]. Thus, we obtain relations for so-called *pseudocritical* values of pressure, temperature, volume, acentric factor, compressibility and density. Generally, the relations are valid for a N-component mixture with x_i being the molar fraction of a constituent.

$$p_c = \sum_i^N x_i\, p_{c\,i} \qquad T_c = \sum_i^N x_i\, T_{c\,i} \qquad 4.1$$

$$V_c = \sum_i^N x_i\, V_{c\,i} \qquad \omega_c = \sum_i^N x_i\, \omega_{c\,i}$$

$$Z_c = \sum_i^N x_i\, Z_{c\,i} \qquad \rho_c = \frac{1}{V_c}$$

Once we obtain these pseudocritical values, they can be directly plugged into an EOS. However, this rather fast and estimative mixing rule is valid under a questionable hypothesis that components within a mixture are not interacting. In other words, such a drawback can be harmlessly neglected for small, non-polar and non-associating molecules only. To conclude, Kay's rule can be used safely for mixtures of non-associating gases (e.g. N_2) and/or gases with similar molecules, such are members of homologous series, perfluorocarbons in our case (C_2F_6 and C_3F_8) [6].

For a mixture of N ideal gases an *apparent* heat capacity ${C_{p,V}}^o(T)$ is calculated as a sum of each compound's proper ${C_{p,V,i}}^o(T)$ weighted by its molar fraction x_i. This formula will be used to calculate mixture heat capacity.

$${C_{p,V}}^o(T) = \sum_{i=1}^N x_i\, {C_{p,V,i}}^o(T) \qquad [\,\mathrm{J.mol^{-1}.K^{-1}}] \qquad 4.2$$

4.3 Real mixture of real gases: Interaction coefficients

Later on, other more precise mixing rules were developed, with applicability extended to real mixtures of real gases. Despite having various forms of arithmetic, geometric or harmonic average, they incorporate a so called binary interaction coefficient k_{ij} [22]. This coefficient describes interaction between i and j components and enables more accurate description of mixture behaviour. The value of the binary interaction coefficient $k_{i=j}=0$ when $i=j$ (a compound does not interfere with itself) and generally is nonzero for $i \neq j$. For our calculations, the value of $k_{ij}=0$ is taken, since the interaction is negligible for hereafter mentioned mixtures of compounds.

Peng and Robinson suggested the usage of following relations (originally derived by Van der Waals for his equation) to calculate parameters in their EOS from parameters a_i and b_i of a pure i-constituent. These mixing rules, visualised in Fig. 7., are used in further calculations. Note that b parameter has form of simple weighted average, whereas a parameter has more complex form.

$$a = \sum_{i}^{N} \sum_{j}^{N} x_i x_j \sqrt{a_i a_j} \left(1 - k_{ij}\right) \qquad [Pa.m^6.mol^{-2}] \qquad 4.3$$

$$b = \sum_{i}^{N} x_i \, b_i \qquad [m^3.mol^{-1}] \qquad 4.4$$

Nevertheless, this basic method is questioned in [7] (bearing in mind a specific application in calculating solubility in supercritical fluids). Here the authors correctly point out that the accuracy of an EOS is essentially limited by the accuracy of used coefficients. They suggest that every EOS should have its own mixing rules properly derived from statistical-mechanical theory and they do so for the Peng-Robinson and Redlich-Kwong EOS.

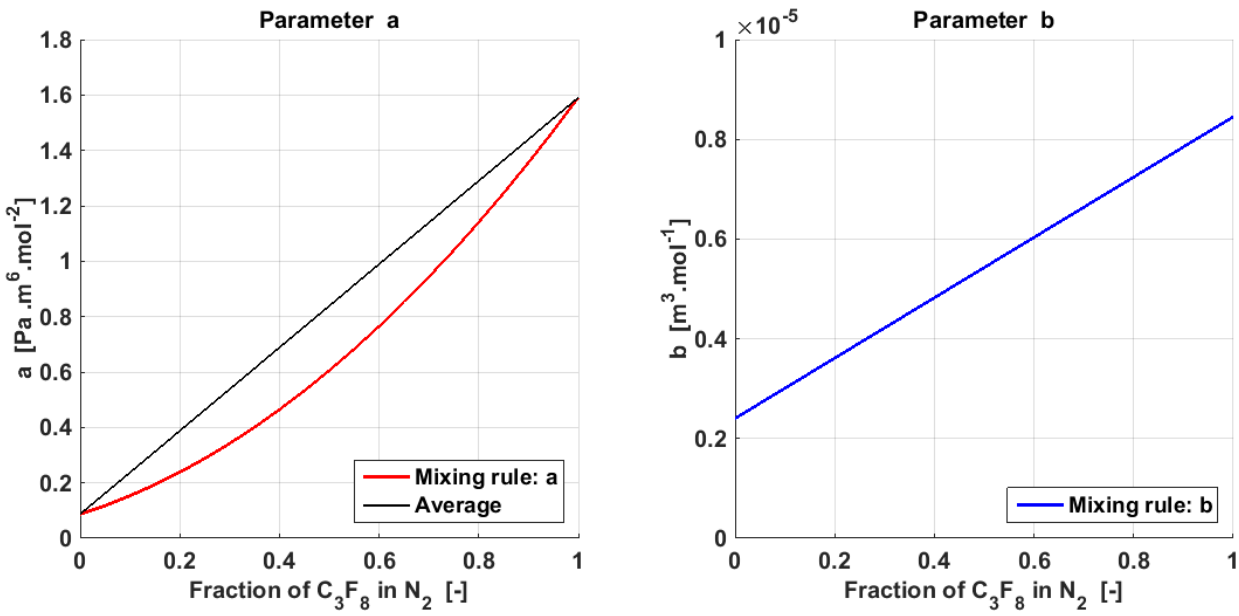

Fig. 7.: Mixing rules. Mixture parameters for various compositions of binary mixtures (C_3F_8 in N_2). Interaction coefficient is neglected: $k_{ij}=0$.

5 Speed of sound in a mixture using Peng-Robinson EOS

5.1 Outline

The calculation of speed of sound in a mixture of real gases consists of multiple separate steps. Firstly, the EOS's derivatives must be calculated, as they take part in the equation for speed of sound and are needed to evaluate the (residual) heat capacity of mixture. Secondly, the heat capacities are evaluated. At last, the apparent molar weight of mixture is determined. This application of Peng-Robinson EOS and the manner of SOS calculation in a mixture of real gases was thoroughly described by R. M. Pratt in [11].

$$c = V_m \sqrt{\frac{C_p}{C_V}\frac{1}{M}\left(\frac{\partial p}{\partial V_m}\right)_T} \qquad [\,\mathrm{m.}\,s^{-1}] \qquad 5.1$$

5.2 Equation of state derivatives

The derivatives of EOS are needed in many calculations of our interest, such as the residual isochoric heat capacity ${C_V}^R$ or the speed of sound *c.*

$$\left(\frac{\partial p}{\partial V_m}\right)_T \qquad \left(\frac{\partial T}{\partial p}\right)_{V_m} \qquad \left(\frac{\partial V_m}{\partial T}\right)_p \qquad 5.2$$

These derivatives take different form for each EOS. In general, a real gas EOS is explicit for the pressure p and implicit for the volume V_m and temperature T. Given this, it is relatively easy to take the two derivatives involving pressure, yet quite arduous to solve the last derivative $\partial V_m/\partial T$. To avoid the calculation of this derivative, we use the triple product rule, which allows us to evaluate one of the 3 derivatives from the remaining two. (This calculus property is only valid if one variable is held constant while differentiating the other two variables.)

$$\left(\frac{\partial p}{\partial V_m}\right)_T \left(\frac{\partial T}{\partial p}\right)_{V_m} \left(\frac{\partial V_m}{\partial T}\right)_p = -1 \qquad [1] \qquad 5.3$$

Peng-Robinson equation is written in the pressure explicit form as usual.

$$p = \frac{R\,T}{V_m - b} - \frac{\mathrm{a}(T)}{V_m(V_m + b) + b(V_m - b)} \qquad [\mathrm{Pa}] \qquad 5.4$$

We can take the two partial derivatives involving the pressure.

$$\left(\frac{\partial p}{\partial T}\right)_{V_m} = \frac{R}{V_m - b} - \frac{a'(T)}{V_m(V_m + b) + b(V_m - b)} \qquad [\mathrm{Pa.\,K^{-1}}] \qquad 5.5$$

$$\left(\frac{\partial p}{\partial V_m}\right)_T = -\frac{R\,T}{(V_m - b)^2} + \frac{2a(V_m + b)}{[V_m(V_m + b) + b(V_m - b)]^2} \qquad [\mathrm{Pa.\,m^{-3}.\,mol^{-1}}] \qquad 5.6$$

Then, using the triple product rule, the remaining partial derivative can be calculated as a ratio of the other two derivatives.

$$\left(\frac{\partial V_m}{\partial T}\right)_p = \frac{-1}{\left(\frac{\partial p}{\partial V_m}\right)_T \left(\frac{\partial T}{\partial p}\right)_{V_m}} = \frac{\left(\frac{\partial p}{\partial T}\right)_{V_m}}{\left(\frac{\partial p}{\partial V_m}\right)_T} \qquad [\mathrm{m}^3.\mathrm{K}^{-1}.\mathrm{mol}^{-1}] \qquad 5.7$$

5.3 Peng Robinson EOS for mixtures

In order to evaluate the Peng-Robinson state equation for a mixture of N gases, we calculate the mixture parameters a and b using some basic mixing rules. Given a vector $\boldsymbol{x_N}$ of constituents molar fractions and also having vectors $\boldsymbol{a_N}$ and $\boldsymbol{b_N}$, we calculate parameters separately for each constituent (with an interaction coefficient $k_{ij} = 0$), and then combine them according to the equations (5.12,5.13).

$$b_i = 0.00777961\,\frac{R\,T_{c\,i}}{p_{c\,i}} \qquad [m^3.mol^{-1}] \qquad 5.8$$

$$a_i(T) = \alpha_i(T)\,0.45723552\,\frac{R^2\,{T_{c\,i}}^2}{p_{c\,i}} \qquad [Pa.m^6.mol^{-2}] \qquad 5.9$$

$$\alpha_i = \left[1 + m_i\,.\left(1 - \sqrt{T/T_{c\,i}}\right)\right]^2 \qquad [1] \qquad 5.10$$

$$m_i = 0.374646 + 1.54226\,\omega_i - 0.26992\,{\omega_i}^2 \qquad [1] \qquad 5.11$$

We can now summarize them into the mixture parameters a and b using these mixing rules.

$$a(T) = \sum_i^N \sum_j^N x_i\,x_j\,\sqrt{a_i(T)\,.\,a_j(T)} \qquad [Pa.m^6.mol^{-2}] \qquad 5.12$$

$$b = \sum_i^N x_i\,b_i \qquad [m^3.mol^{-1}] \qquad 5.13$$

The b parameter is a constant, whereas the a parameter is *temperature dependent*, implying that while taking the derivatives of the Peng-Robinson EOS, we have to derive each component's a_i as well. The 1st derivative is needed to calculate the speed of sound and 2nd derivative to evaluate the residual heat capacity of a mixture. The relation for $a'(T)$ of mixture is the following.

$$a'(T) = \frac{1}{2}\sum_i^N \sum_j^N x_i\,x_j\left(\sqrt{\frac{a_j}{a_i}}.\,{a_i}' + \sqrt{\frac{a_i}{a_j}}.\,{a_j}'\right) \qquad [Pa.m^6.mol^{-2}.K^{-1}] \qquad 5.14$$

With component's $a_i'(T)$ as follows.

$$a_i'(T) = \frac{-m.a_i}{\left[1 + m_i(1 - \sqrt{T/T_{c\,i}}\right]\sqrt{T.T_{c\,i}}} \qquad [Pa.m^6.mol^{-2}.K^{-1}] \qquad 5.15$$

The 2nd derivative $a''(T)$ of a mixture is

$$a''(T) = \frac{1}{2}\sum_i^N \sum_j^N x_i\, x_j \left[\frac{a_i'a_j' + a_i''a_j + a_i a_j''}{\sqrt{a_i a_j}} - \frac{1}{2}\left(\sqrt{\frac{a_j}{a_i^3}}\, a_i'^2 + \sqrt{\frac{a_i}{a_j^3}}\, a_j'^2\right)\right] \qquad 5.16$$

With component's $a_i''(T)$ as follows.

$$a_i''(T) = \frac{a_{c\,i}\,(m_i + m_i^2)\,\sqrt{T_{c\,i}/T}}{2.T.T_{c\,i}} \qquad [Pa.m^6.mol^{-2}.K^{-2}] \qquad 5.17$$

The corectness of these derivatives was checked numerically, to eliminate possible source of error. Now we have the mixture parameters needed for evaluating the PR EOS derivatives, which play role in the speed of sound calculation. Moreover, we derived the $a''(T)$, which is necessary for calculating the residual isochoric heat capacity ${C_V}^R$ of a mixture and has the following form.

$${C_V}^R(T) = \frac{T.a''(T)}{\sqrt{8}\,b}\,\ln\left[\frac{Z + B(1+\sqrt{2})}{Z + B(1-\sqrt{2})}\right] \qquad [\,\mathrm{J.mol^{-1}.K^{-1}}] \qquad 5.18$$

6 Group contribution methods

6.1 Introduction

All of the above-mentioned equations need to be provided with various parameters. For a number of basic compounds these parameters (critical point, acentric factor, heat capacities, etc.) were measured and tabulated. Yet, for many compounds and especially the complex ones, these properties are often inaccessible. As Marrero and Gani [10] state: "It is not always possible, however, to find experimental values of properties for the compounds of interest in the literature. Since, it is not practical to measure them as the need arises, estimation methods are generally employed in this and other similar situations."

The group contribution methods are generally designed for organic compounds. The reason is that organic compounds are by orders of magnitude more numerous than the inorganic ones and therefore a great part of the organic chemicals have not had their thermodynamic properties investigated, so they need to be determined by other means.

6.2 Basic methods

As Kolská et al. [8] are explaining, these methods work as follows: "Group contribution methods are based on the so called 'additive principle'. That means any compound can be divided into fragments, usually atoms, bonds or group of atoms, etc. All fragments have a partial value called a contribution. These contributions are calculated from known experimental data. Property of a compound is obtained by summing up the values of all contributions presented in the molecule."

Marrero and Gani [10] explain the method similarly, but add some concerns about the accuracy: "In these methods, the property of a compound is a function of structurally-dependent parameters, which are determined by summing the frequency of each group occurring in the molecule times its contribution. These methods provide the advantage of quick estimates without requiring substantial computational resources. Many of these methods are, however, of questionable accuracy, and are unable to distinguish among isomers and have limited applicability due to the oversimplification of the molecular structure representation as a result of the use of a simple group-contribution approach and a relatively small data set used for estimation of group-contributions." Then they introduce a new method, designed to account for the above-mentioned deficiencies.

6.3 Group decomposition

Before proceeding to the calculation of thermodynamic properties of a compound, its chemical formula needs to be decomposed into groups. This can be done in various ways, depending on which method is being used (Fig. 8.). Some former methods, e.g. Joback and Reid use more or less the functional groups known from classical chemistry. In contrast, more recent methods, like that of Constantinou and Gani, already employ structural groups from UNIFAC (UNIversal quasichemical Functional-group Activity Coefficients).

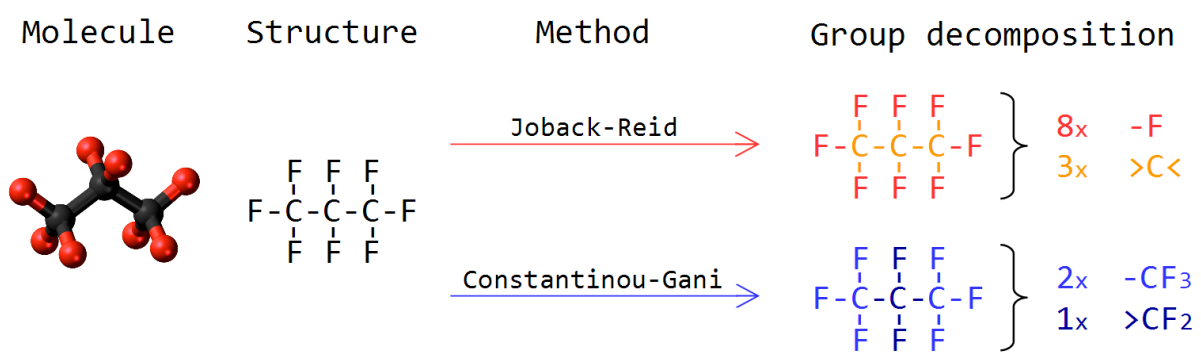

Fig. 8.: Group decomposition. Compound's chemical structure is decomposed according to JR and CG methods.

6.4 Method of Joback and Reid

One of the simplest group contribution methods was presented by Joback and Reid (JR). As published by Poling et al. [9]: "Joback re-evaluated Lydersen's group contribution scheme, added several new functional groups, and determined new contribution values."

In all these equations the individual group contributions intervene in a form of summation. The index i indicates contribution from a single group of ith kind and N_i is the frequency of the ith group in a single molecule of a compound. The relations for critical properties of a pure compound are following. The simplest Joback's relation is that for the boiling point temperature T_b [K], whereas the critical properties are described by more complex formulas.

$$T_b = \left[198 + \sum_i N_i\, T_{b,i}\right] \qquad [K] \qquad 6.1$$

$$T_C = T_b.\left[0.584 + 0.965\left[\sum_i N_i\, T_{C,i}\right] - \left[\sum_i N_i\, T_{C,i}\right]^2\right]^{-1} \qquad [K] \qquad 6.2$$

$$p_C = 0.1\ .\left[0.113 + 0.0032\,.N_A - \sum_i N_i\, p_{C,i}\right]^{-2} \qquad [MPa] \qquad 6.3$$

$$V_C = \left[17.5 + \sum_i N_i\, V_{C,i}\right].10^{-3} \qquad [m^3.kmol^{-1}] \qquad 6.4$$

For the isobaric molar heat capacity of a pure ideal gas C_p^o [J.mol^{-1}.K^{-1}] a 3rd degree polynomial has been established.

$$\begin{aligned} C_p^o = \quad & (-37.93 + \sum_i N_i\, a_i) \\ & +(\,0.21 + \sum_i N_i\, b_i).T \\ & +(-3.91\,.10^{-4} + \sum_i N_i\, c_i).T^2 \\ & +(-2.06\,.10^{-7} + \sum_i N_i\, d_i).T^3 \end{aligned} \qquad [\,\mathrm{J.mol^{-1}.K^{-1}}] \qquad 6.5$$

6.4.1 Application of Joback and Reid method

Two perfluorocarbon (PFC) compounds C_2F_6 and C_3F_8 were chosen to demonstrate the JR method, as their properties are needed further on to be compared with the measurements. The chemicals are decomposed into groups as defined in tables created by Joback and Reid, and their relative contributions are read out (Table 3). Then, all contributions are multiplied by their frequency of occurrence in a molecule, added together and plugged into the formulas 6.1-6.5, resulting into the desired properties. These are to be found in Table 5., as well as values from NIST database for comparison.

Table 3.: Joback's coefficients for acyclic carbon ">C<" and fluorine "-F". Retrieved from [9].

Group	$T_{b,i}$	$T_{C,i}$	$p_{C,i}$	$V_{C,i}$	a_i	b_i	c_i	d_i
>C<	18.25	6.7e-3	4.3e-3	27	-6.62e1	4.27e-1	-6.41e-4	3.01e-7
-F	-0.03	-5.7e-3	1.11e-2	28	2.65e1	-9.13e-2	1.91e-4	-1.03e-7

6.5 Method of Constantinou and Gani

The Constantinou and Gani method works similarly to JR method and even though the equations 6.6-6.10 employ different mathematical functions, the method is still based on the same principle of linear contribution of individual groups to the final property.

The method consist of two steps. In the first step the concerned organic molecule is decomposed into functional groups of so-called 1st order (Fig. 8). Their partial contributions are read out from tables, summarized and put into the equations 6.6-6.10, resulting into the desired properties. The parameter *w = 0* for the 1st order calculation.

Then, if the organic molecule is complex and contains more functional groups, the *w* parameter is set equal to *1* and the 2nd order of the CG method comes into act. Again, the molecule is subdivided into groups, yet this time they are larger than the 1st order ones. The 2nd order approximation is designed to account for the proximity effect amongst 1st order groups and to make a correction for e.g. rings of carbon atoms, or specific chains abundant in the molecule.

$$T_b = 204.359 \,.\, \ln\left(\sum_i N_i\, T_{b,N,i} + \mathrm{w}.\sum_j M_j\, T_{b,M,J}\right) \qquad [K] \qquad 6.6$$

$$T_\mathrm{c} = 181.128 \,.\, \ln\left(\sum_i N_i\, T_{c,N,i} + \mathrm{w}.\sum_j M_j\, T_{c,N,i}\right) \qquad [K] \qquad 6.7$$

$$p_\mathrm{c} = 0.1 \,.\left[1.3705 + \left(\sum_i N_i\, \mathrm{p}_{c,N,i} + \mathrm{w}.\sum_j M_j\, \mathrm{p}_{c,M,j} + 0.10022\right)^{-2}\right] \qquad [MPa] \qquad 6.8$$

$$V_\mathrm{c} = -0.00435 + \left(\sum_i N_i\, \mathrm{V}_{c,N,i} + \mathrm{w}.\sum_j M_j\, \mathrm{V}_{c,M,j}\right) \qquad [m^3.kmol^{-1}] \qquad 6.9$$

$$\begin{aligned} \mathrm{C}_p^o = & \left(\sum_i N_i\, a_{N,i} + \mathrm{w}.\sum_j M_j\, a_{M,j} - 19.7779\right) \\ & + \left(\sum_i N_i\, b_{N,i} + \mathrm{w}.\sum_j M_j\, b_{M,j} + 22.5981\right).\Theta \\ & + \left(\sum_i N_i\, c_{N,i} + \mathrm{w}.\sum_j M_j\, c_{M,j} - 10.7983\right).\Theta^2 \end{aligned} \qquad [\,\mathrm{J.mol^{-1}.K^{-1}}] \qquad 6.10$$

Where parameter Θ is a function of temperature: $\Theta = \frac{T-298}{700}$ $[K]$ *6.11*

6.5.1 Application of Constantinou and Gani method

Since the compounds of our concern (C_2F_6 and C_3F_8) are quite simple, they do not have the 2nd order correction in the tables of the CG method, we can set the *w = 0* and calculate the 1st order approximation only. Despite that, the results of CG method are fairly accurate when compared to the NIST database and certainly more accurate than the JR method. The calculation itself resembles the case of Joback's method.

Table 4.: Coefficients of Constantinou and Gani method for groups -CF₃ and >CF₂ needed to evaluate properties of our two comcpounds. Values are retrieved from [9].

Group	$T_{b,N,i}$	$T_{c,N,i}$	$p_{C,i}$	$V_{C,i}$	$a_{N,i}$	$b_{N,i}$	$c_{N,i}$
$>CF_2$	0.6115	1.7399	0.0129	0.0952	44.3567	44.5875	-23.2820
$-CF_3$	1.2880	2.4778	0.0442	0.1148	63.2024	51.9366	-28.6308

6.6 Accuracy of methods compared to NIST database

The following Table 5. shows compounds' properties as estimated by the JR and CG group contribution methods. These values are then compared to the NIST database values and the average absolute deviation (AAD) is calculated at the bottom line. It is obvious, that on these two compounds, the CG method is by an order of magnitude more accurate than the JR method and approaches the NIST database values within a couple of percents.

Table 5.: Thermodynamic properties of C_2F_6 and C_3F_8 as calculated by JR and CG methods are compared to NIST REFPROP database. AAD: Average Absolute Deviation [%] of contribution methods as compared to NIST.

Property		Compound					
		C_2F_6 (R116)			**C_3F_8 (R218)**		
		Method/Source			Method/Source		
		JR	CG (1°)	NIST	JR	CG (1°)	NIST
T_b	[K]	234.3	193.4	195.1	252.5	236.9	236.4
T_C	[K]	357.8	289.9	293.0	372.9	344.4	345.0
p_C	[MPa]	3.709	2.948	3.048	3.056	2.600	2.640
$V_{m,C}$	[m^3/kmol]	0.234	0.225	0.225	0.314	0.3205	0.299
ρ_C	[kg/m^3]	591.06	612.71	613.32	597.8	586.7	627.98
${C_p}^o$(T = 300 K)	[J/mol. K]	101.23	106.99	106.82	140.6	151.5	148.54
AAD	[%]	12.76	0.93	-	7.64	2.94	-

6.7 Literature research conclusion

While reviewing the accuracy of various state equations, it was found out that the Peng-Robinson state equation suits best our application (concerning heavier compounds present in the mixtures). Globally, the PR EOS features greater versatility and it is a good trade-off between accuracy and complexity.

To make use of the full potential of the PR state equation and to achieve the best accuracy, it was chosen to employ the NIST database thermodynamic properties for critical point and acentric factor. If the database values were inaccessible, then the properties obtained from group contribution methods could be used and one would still get decent results.

7 MATLAB implementation

MATLAB programming language was used to implement the theoretical model described above. In order to use this code beyond the extent of this work, it was chosen to divide the code into multiple functions. One for each of the separate tasks in evaluating the mixture SOS. This is to provide certain amount of modularity, and reusability. The emphasis was put on effectivity of the code, but also on a fool-proof behaviour. Simplified scheme of the implementation is put forward in order to explain its manner of work.

7.1 Group contribution methods

MATLAB functions *JR.m*, *CG.m* (and *NIST.m*) ware programmed in order to evaluate the two previously mentioned group contribution methods. When one of these functions is given a compound, it sums the individual group contributions and returns the compounds' thermodynamic properties (Fig. 9). The function *PR_params.m* calls one of the methods, giving compound's formula as an argument and receiving the compounds properties as a vector of variables. As a result, this calling function obtains compounds' thermodynamic properties at the critical point values $\boldsymbol{T_C}$, $\boldsymbol{p_C}$, $\boldsymbol{V_C}$ estimated by the chosen method and coefficients of a 3rd degree polynomial of ideal heat capacity $\boldsymbol{C_p^o}$.

All the functions use an excel spreadsheet *Coefs.xls* to store table values as they were retrieved from the work of Poling et al. [9], or from NIST REFPROP database [6]. These tables were partially rewritten in Table 3. and Table 4. Unfortunatelly, neither of the contribution methods employs basic SI units, so the results are converted into SI to avoid unit bias in further calculations.

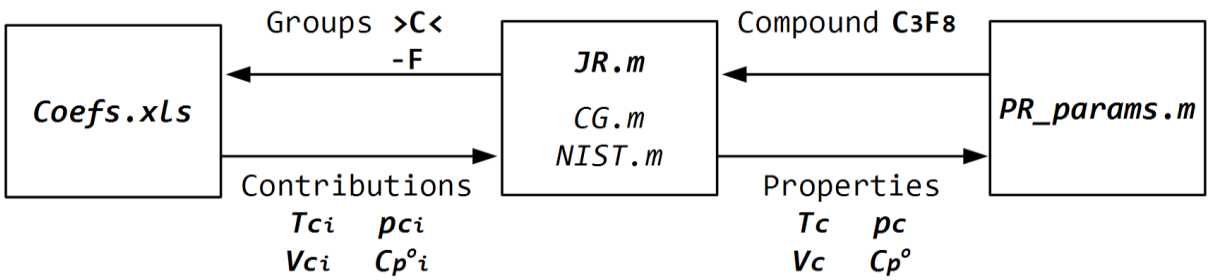

Fig. 9.: Multi-level structure of MATLAB code. Note the flow of variables between the functions. The function PR_params.m obtains properties of a desired compound using a chosen method.

7.2 Mixture parameters for Peng-Robinson equation

Function *PR_mix.m* is given the compounds' properties by *PR_params.m*. Then it employs mixing rules to calculate the parameters **a** and **b** of the concerned mixture, that are needed for evaluating the Peng-Robinson EOS. It also evaluates its derivatives, as well as the 'apparent' (or 'pseudo') molar mas $\boldsymbol{M}$ and heat capacity $\mathbf{C_p^o}(\boldsymbol{T})$ of mixture. The 3rd state variable $\boldsymbol{\rho}$ was solved analytically from the PR EOS

to accelerate the calculation. Now that all the values needed for SOS calculation are known, it can be rendered to the user. Finally, the *SOS.m* function compares the theoretical results with measurement and plots the results. The processing of measured data will be described in the next chapter.

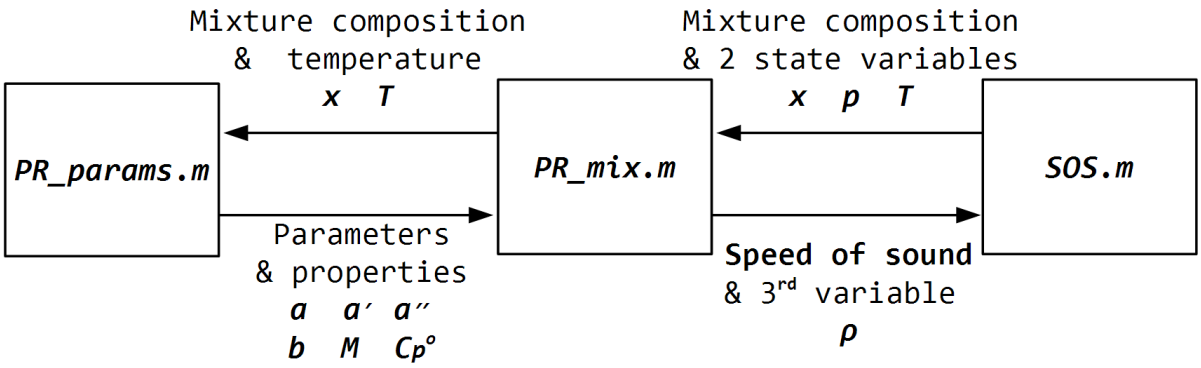

Fig. 10.: Structure of MATLAB code. The speed of sound is calculated for a given pressure, temperature and composition

7.3 Speed of sound calculation

The Fig. 11 visualises the results of an example calculation. At the first place it shows the importance of proper mixing rules. Note that the value of speed of sound in a mixture is far from being a simple weighted average of the pure components. The chosen temperatures are in fact the ambient temperature and highest and lowest temperatures reached during the measurement. The pressure is held constant at 1 bar, eventhough the speed of sound does not vary greatly with pressure. Remark that the SOS increases with rising temperature, because the molecules' mean velocity, which is responsible for the sound wave propagation, increases as well.

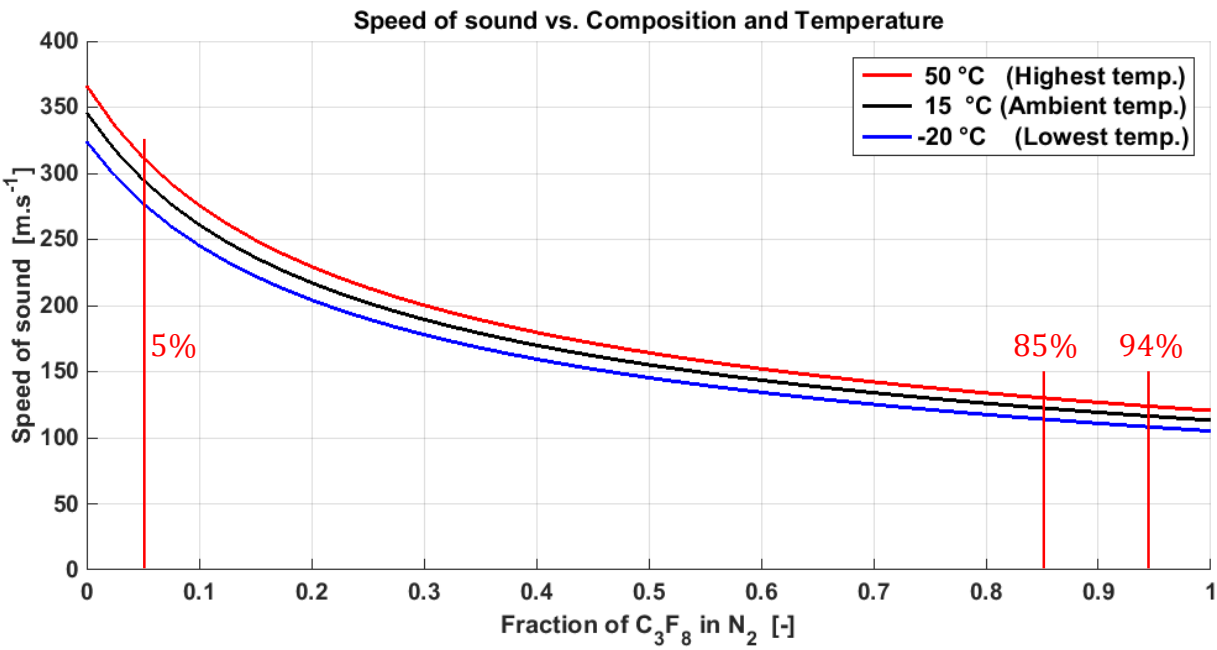

Fig. 11.: Speed of sound in a mixture vs. Composition and Temperature. The pressure is set to 0.1 MPa in the calculation. Approximate position of measured mixtures is marked by red lines.

8 Measurement

8.1 Introduction

Given the motivation mentioned in the introductory part and the theory described and derived above, it is now desirable to confront the analytical solution with an experimental data. To provide a dataset for comparison, a measurement was performed on the sonar tube experimental setup. It was developed at the Department of Physics at the Faculty of Mechanical Engineering at the CTU in Prague, which has great experience in this field [17,18,19]. This particular design of the apparatus and read-out electronics, as well as calibration and commissioning procedure was thoroughly described in theses of M. Doubek [13, 14].

8.2 Experiment setup

8.2.1 Principle

There are different of methods for measuring the speed of sound, using resonance or interference of a soundwave, or emplying the principle of sonar. This method, consisting essentially of measuring transition time of a sound wave between two points, was carefully chosen amongst the other schemes. The principle of the measurement is apparent from the scheme in Fig. 13. The sound wave propagates over the calibrated distance (0.5 m) and the transition time is measured by a counter. Then the SOS is calculated from these two values. Since the sonar tube forms an enclosed volume, the pressure in the tube varies along with temperature, making it an isochoric process.

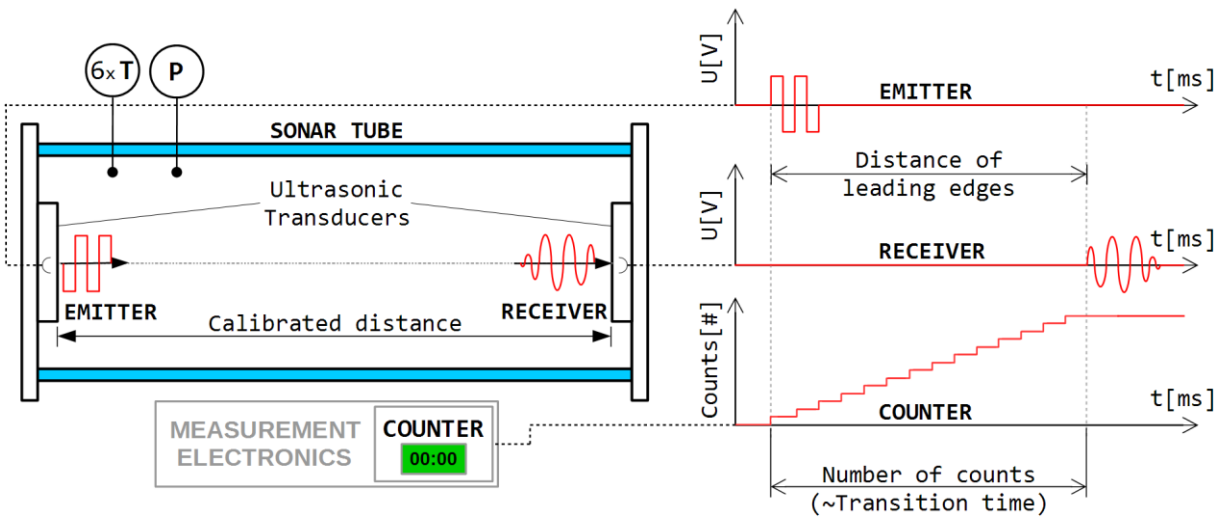

Fig. 12.: Simplified scheme of transition time measurement. The time between the leading edges of emitted and received signal is measured by a 20MHz counter, which makes part of the measurement electronics.

8.2.2 Construction

The investigated gas is enclosed in a sonar tube, where the measurement of unidirectional sound wave propagation takes place. The inner volume, formed by steel tube with flanges on both sides, can enclose hermetically the investigated gas up to a pressure of 5 bar_a. The construction is also capable of maintaining vacuum, but for the pressures below 0.2 bar_a , the ultrasaund does not propagate enough to be detected. The pressure transducer Keller 33X is connected via feedthrough mounted in flanges, whereas the read-out electronics and temperature sensors (NTC and Pt1000) are connected through cable connectors. Double-walled steel cylinder is used to provide liquid cooling/heating of the inner cell volume. This cooling jacket is connected to a chiller, which operates at temperatures between -20°C and +50°C (± 0.5 °C) by pumping the cooling liquid (glycol in our case) through a closed circuit.

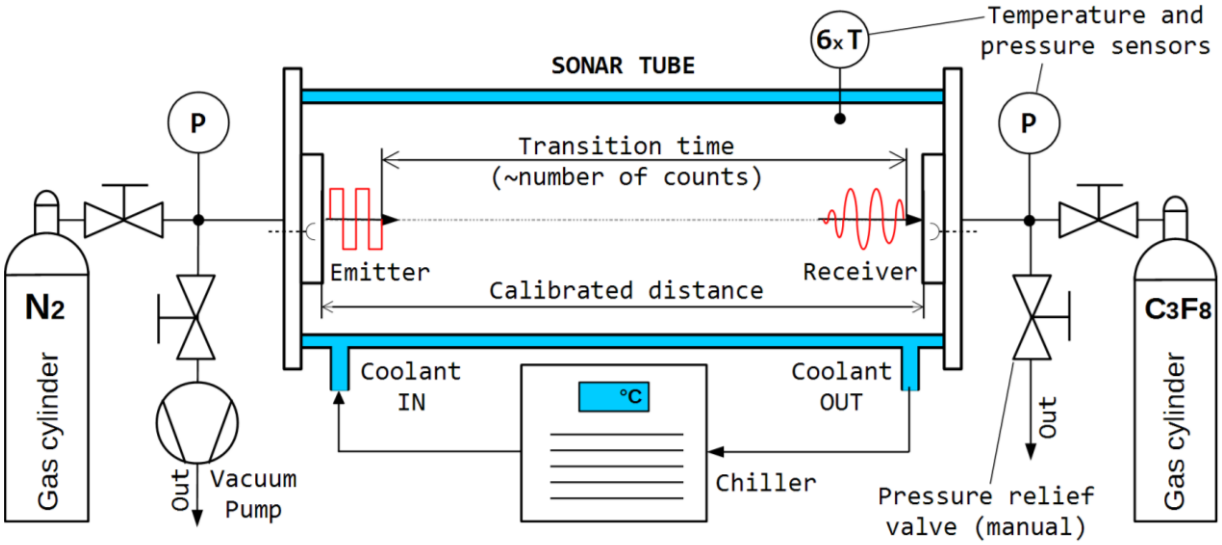

Fig. 13.: Scheme of the measurement hardware. Note the gas cylinders, valves, vacuum pump and tubing with mounted pressure sensors. Also note the chiller pushing the coolant through double walled sonar tube.

8.3 Data acquisition

Ultrasound wave with frequency of 50 kHz is emitted by a transmitter on one side of the tube, it propagates over the calibrated distance, through a medium with known pressure and temperatrure and is then captured by the receiver on the other side. The emitting and receiving devices are the same (thus interchangeable) and are realized by the SensComp 600 capacitive ultrasonic transducers. The gold coated diaphragm is enclosed in stainless steel housing. They feature a narrow beam pattern and despite of having flat frequency response, they are operated at their nominal frequency of 50 kHz.

Fig. 14.: SensComp 600 ultrasonic capacitive transducer. Gold foil enclosed in stainless steel casing features chemical inertness.

Measurement of the transition time is realized by the 20 MHz counter which starts with the leading edge of the emitted signal and is stopped once the pulse reaches the receiver. Precisely when the read-out electronics of the receiver detects the leading edge of the incoming signal. As described in [14], there is a very refined manner of the leading edge detection. It distinguishes the incoming leading edge before it even surpasses the noise level, but at the same time omits false positives. Finally, knowing the length of one tick of the counter (20 ms), the number of counts is converted into transition time.

Approximate geometrical distance between the transducers was correted by measuring the transition time in pure N_2 gas. This transition time was then multiplied by nitrogen's well-known sound speed to obtain a *virtual distance*, that was traveled by the signal between its emission and reception. Despite its rather abstract nature, this definition of distance enables greater precision, because it accounts not only for geometrical imperfections but also for response time of read-out electronics.

Pressure and temperature are measured directly. The NTC and Pt1000 temperature sensors are positioned inside the tube along the path of the sound-wave (but not interfering it). The pressure is measured by the Keller 33X absolute pressure sensor with nominal accuracy of 0.3 mbar. These sensors and electronics are connected to a data acquisition (DAQ) PC using RS-232 and USB interfaces. The DAQ PC runs WinCC OA software (formerly PVSS), which controls the whole process of measurement and ensures communication between chiller, electronics and *p-T* sensors. The DAQ PC controls the chiller, which heats up or cools down the sonar tube to desired temperature setpoints. Then it performs measurements on a stabilised system and stores the measured data in a database.

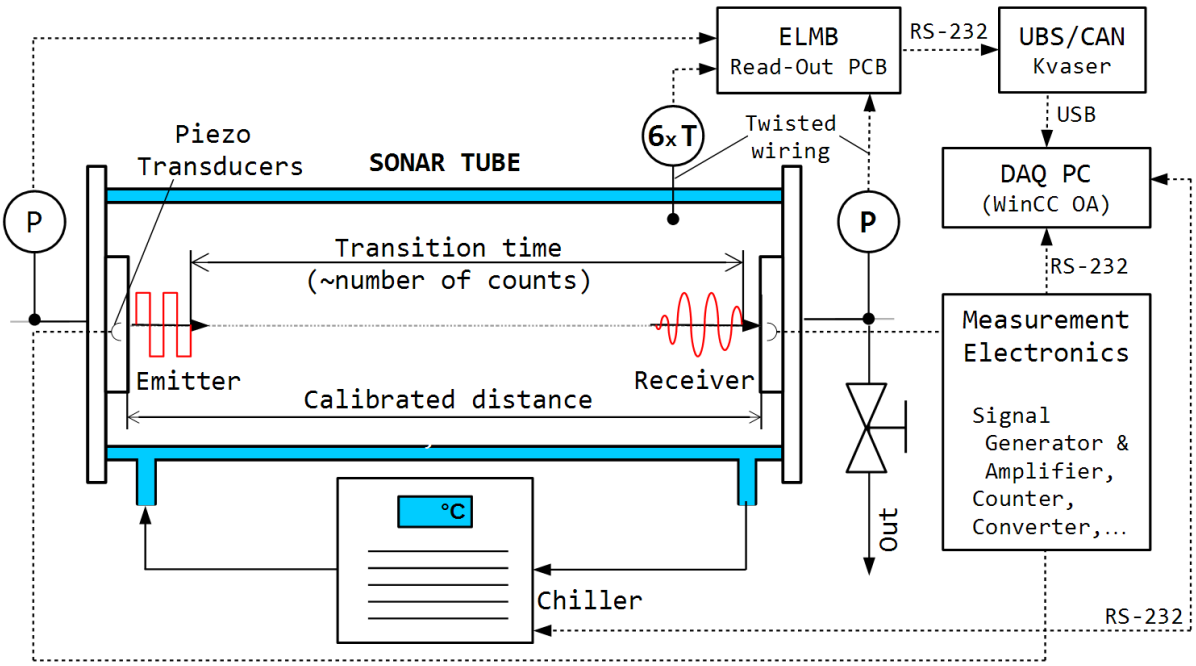

Fig. 15.: Scheme of electronics and instrumentation. Notice the measurement electronics and ELMB read-out board, which are both connected to the DAQ PC through serial port RS-232. The temperature and pressure sensors are all connected by twisted wiring to avoid interference.

8.4 Measurement procedure

8.4.1 Emptying the sonar tube

Before the measurement can begin, the sonar tube needs to be emptied from gases remaining from previous measurements, or maintenance. This is done using arotary vane vacuum pump. The inner volume of sonar tube is then flushed with a small amount of N_2 and vacuumed again. The nitrogen gas was chosen in this case, because it is a constituent of mixtures investigated in further measurements. Moreover, it is a cheap industrial gas with well-known properties. This procedure is repeated twice to ensure purity of the device before proceeding to the mixing itself.

8.4.2 Defining a mixture

To create a desired mixture of N gases, its composition has to be known in terms of molar fractions x_i. Molar fractions of constituents have to summarize into 1.

$$\sum_i^N x_i \equiv 1 \qquad [-] \qquad 8.1$$

One calculates the constituents' partial pressures by exploiting the Dalton's law, which states that the total pressure of a gas mixture is a sum of partial pressures of its constituents. The gases are then added one after other into the sonar tube and in the end these partial pressures summarize into the total pressure in the tube.

$$p_{total} = \sum_i^N p_i \qquad [Pa] \qquad 8.2$$

$$p_i = x_i \cdot p_{total} \qquad [Pa] \qquad 8.3$$

These relations can be simplified for a binary mixture of A and B constituents.

$$x_A + x_B \equiv 1 \qquad [-] \qquad 8.4$$

$$p_A + p_B = p_{total} \qquad [Pa] \qquad 8.5$$

$$p_A = x_A \cdot p_{total} \qquad [Pa] \qquad 8.6$$

$$p_B = x_B \cdot p_{total} = (1 - x_A) \cdot p_{total} \qquad [Pa] \qquad 8.7$$

8.4.3 Creating a mixture

Given the (desired) partial pressures $p_{A,B}$, the first constituent is let from a gas cylinder inside the previously evacuated sonar tube. The tube is then filled with A constituent up to a pressure, which is equal to constitutent's partial pressure p_A in the desired mixture.

Then, the second compound is added into the sonar tube, until reaching the total pressure p_{total}. When letting the gas from a gas cylinder into the tube, the gas undergoes an expansion, thus cools down. To ensure accurate composition,

the pressures have to be measured at the same temperature, so the system requires stabilisation (≈10min) before the partial pressure is read out.

When the mixture is ready, the measured p-T data through the course of the mixing process is exported. Finally, the actual composition $x_{A,B}^{real}$ of a binary mixture is calculated from the pressures p^m measured at a constant temperature T.

$$x_A{}^{real} = \left(\frac{p_A^m}{p_{total}^m}\right)_T \qquad [-] \qquad 8.8$$

$$x_B{}^{real} = \left(\frac{p_{total}^m - p_A^m}{p_{total}^m}\right)_T \equiv 1 - x_A{}^{real} \qquad [-] \qquad 8.9$$

8.4.4 Measurement of an isochore

Once the well defined mixture is hermetically enclosed in the sonar tube (constant volume), the measurements can be taken. On the DAQ PC, a process responsible for communication with the chiller is run from the application's task manager. This process opens a graphical user interface, through which a user loads a list of temperature setpoints. As can be seen Fig. 16, the setpoints are arrayed in an up-down step-wise function, so every setpoint is measured twice, once reaching the target temperature from above, once from below (except for marginal values). That is done to prevent the hysteresis effect in the measurement. The total of 31 setpoints is measured, covering range of temperatures from-20°C to +50°C, with steps of 5°C.

When a setpoint is sent to a chiller, it controls the stabilisation of the system on the required temperature within ±0.5 °C. In about 1 hour, when the system

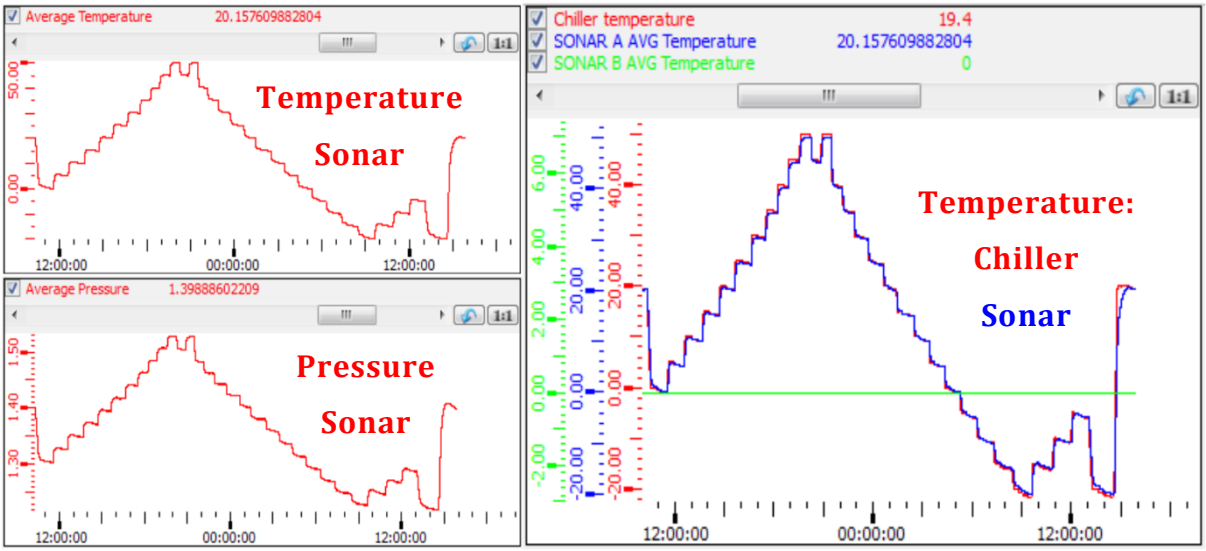

Fig. 16.: GUI in WinCC OA software. The real-time graphical user interface showing progress of temperature (TopLeft), pressure (BottomLeft), and SOS (Right) during one isochore measurement.

stabilises on the target value, the total of 300 read-outs is taken by the DAQ PC, consisting essentially of *p-T* values and number of ticks of the 20 MHz counter. Then the chiller is demanded a new setpoint and the whole process repeats. On Fig. 16 note how accurately the pressure reacts to the temperature changes. This is a consequence of an isochoric process in the tube. On the right side, note the response of sonar (blue) to a step change of chiller (red) temperature.

8.4.5 Measurements at different isochores

The measurement of 1 isochore (consisting of 31 temperature setpoints) takes about 30hours to finish. The data files from each isochore measurement is exported, and immediately processed to see, whether the measurement was performed correctly. If not, it can be repeated.

If the apparatus performed well, then the pressure is relieved (usually by 0.2 bar) using the manual pressure relief valve (Fig. 13), setpoints are reloaded into the chiller-controlling application and the measurement is started again. Next isochore measurement is performed, yet this time with smaller pressure than before, since part of the gas was released into the atmosphere (Fig. 17). The pressure is released after each isochore measurement, until the atmospheric level is reached (at 20 °C). This way, a wide pressure range is covered, starting from pressures even higher than those used for mixing, going down below atmospheric pressure.

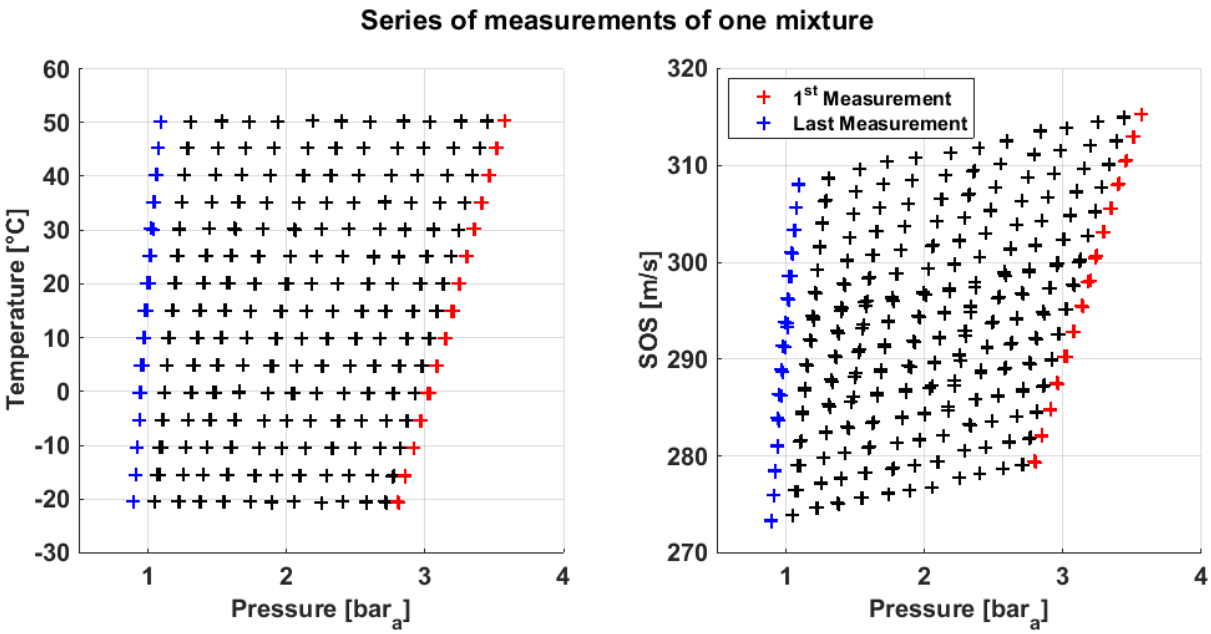

Fig. 17.: Sample measurement of mixture 1 at different pressures. Data was taken for the mixture of 95% N_2 and 5% C_3F_8.

8.5 Data processing

8.5.1 Outline

WinCC OA software creates a *.csv* file for each setpoint measured, containing exactly 300 read-outs. When the measurement is finished, the *.csv* files are processed using MATLAB script. It filters the data, calculates average value and standard deviation and then exports the processed data into a *.xls* file. To obtain more precise results, the temperature dilatation of the tube is also taken into account. The speed of sounds values can be then compared to a theoretical prediction.

8.5.2 Data processing

The measured *.csv* files are loaded into MATLAB. One file at a time, with exactly N_{total} = 300 read-outs is taken and sorted by the number of counts N_i. These two numbers divide into a relative frequency of counts f_i , from which a histogram of counts' occurence is created.

$$f_i = \frac{N_i}{N_{total}} \cdot 100\ \% \qquad [\%] \qquad 8.10$$

Only the counts with frequencies higher than 10% are chosen for further processing, assuming that the real value is located in the middle of the distribution curve. Correspondingly to these chosen values of counts, only their *p-T* values are taken into account, while the rest is neglected. When the data is disposed of insignificant data points, the remaining values are averaged and standard deviation is calculated on this statistical sample.

Such procedure is done for each setpoint of each series of measurement. Finally, this processed data can be plotted and compared to the theoretical prediction.

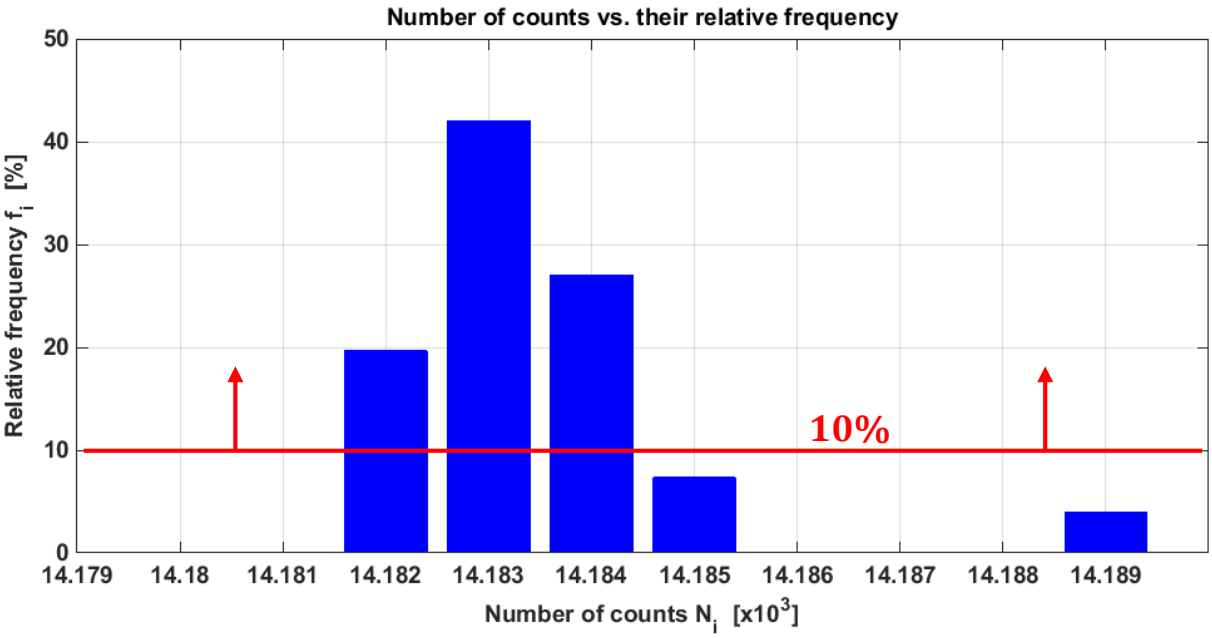

Fig. 18.: Selecting data points using histogram. Only peaks representing abundance greater than 10% are considered to be enough significant to be further processed.

9 Theory and measurement comparison

9.1 Outline

The values of speed of sound measured in mixtures of N_2 with C_3F_8 are now to be compared with the speed of sound calculated analytically using the Peng-Robinson equation of state, which was supplied with NIST thermodynamic properties.

To compare experimental and theoretical data, the relative deviation RD [%] is calculated for each of the data points. Then it is plotted as a function of density.

$$RD\ [\%] = \frac{SOS^{measured} - SOS^{expected}}{SOS^{expected}} \,.100\ \% \qquad [\%] \qquad 9.1$$

9.2 Mixtures of N_2 with C_3F_8

Bearing in mind the application for in-situ measurement of composition of refrigerant, it was chosen to measure the following mixtures of N_2 and C_3F_8 (Table 6). Each has different ratio of constituents, focusing on C_3F_8-rich mixtures, because they simulate contamination of refrigerant with atmospheric air, consisting mostly of N_2. In the case of mixtures with high ratio of C_3F_8 (mixtures 2, 3), the saturation curve was reached and condensation occurred at certain points (high pressure and low temperature). These points were manually removed from the dataset for now, but can be used later to determine part of the saturation curve. The anticipated position of the saturation curve is marked in the Fig. 19, which represents the typical occurrence of condensation during the course of measurement.

Table 6.: Mixtures with different compositions that were measured.

Mixture	Molar fraction x [-]		Achieved interval of correlation between theory and measurement in terms of SOS
	N_2	C_3F_8	
1	0.954	0.046	-2.5% to 0.2%
2	0.063	0.937	-0.2% to 1.5%
3	0.157	0.843	0.8% to 1.8%

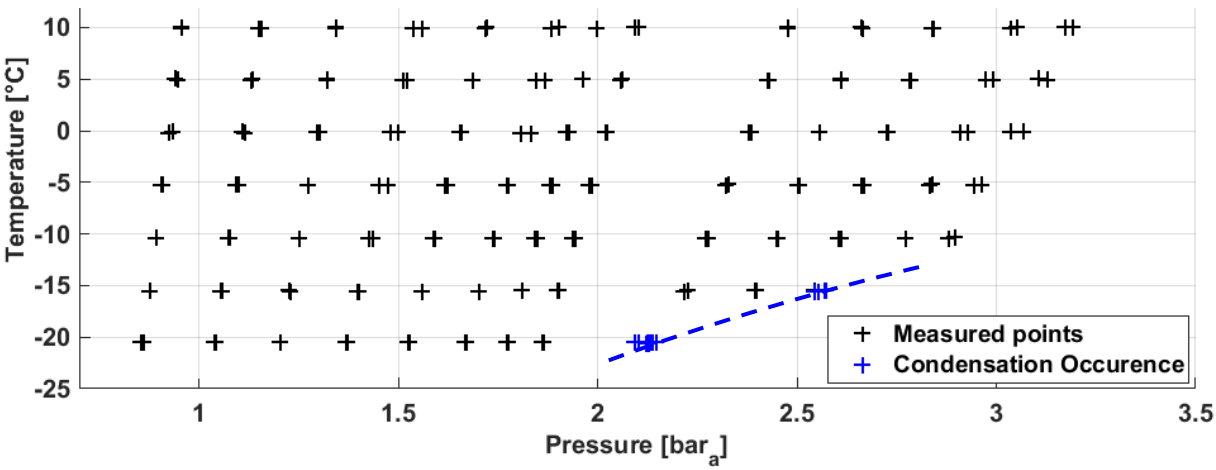

Fig. 19.: Condensation occurrence during measurement of points close to saturation curve. Anticipated position of the saturation curve is approximately marked in the figure. (Mixture 2)

9.3 Mixture 1 (95% N_2 and 5% C_3F_8)

In this mixture consisting mostly of N_2, the theoretical SOS calculated by the developed model is overestimated (Fig. 20). On average it predicts higher SOS than measured. These two plots were subtracted from each other, resulting into Fig. 21. It shows that relative deviation between the theory and measurement is very small for high densities, but SOS differ by as much as 2.5% in the low density region.

This behaviour is very uneexpected and should be further examined, because state equations tend to be more precise in the low density region, where gases

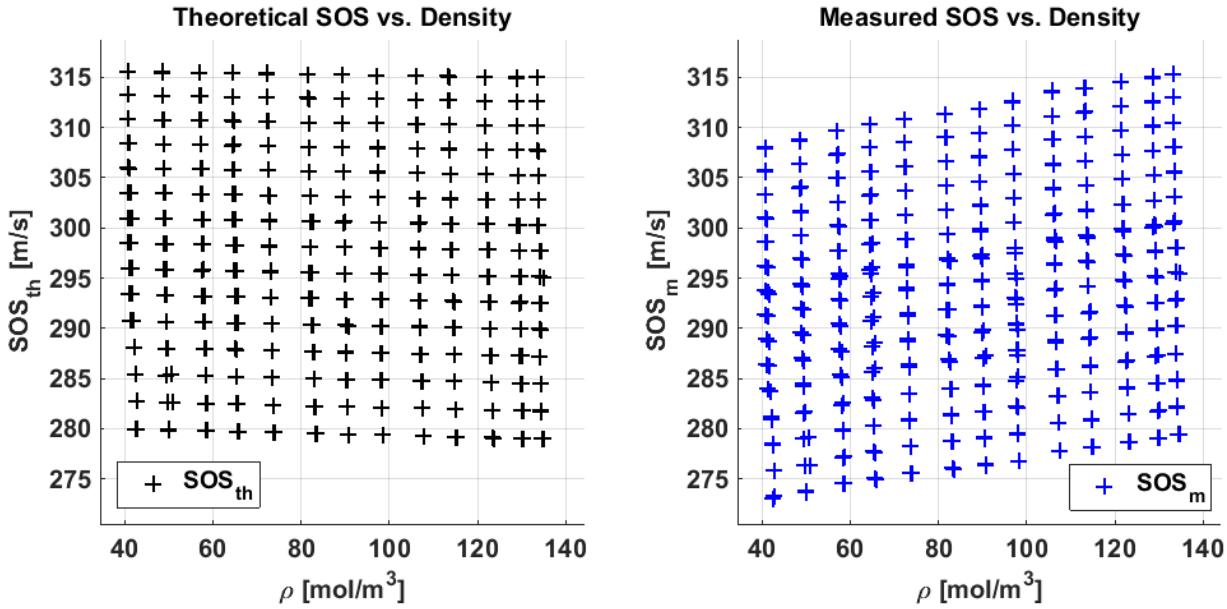

Fig. 20.: Mixture 1 (95% N_2 and 5% C_3F_8). Left: Model prediction. Right: Measured data.

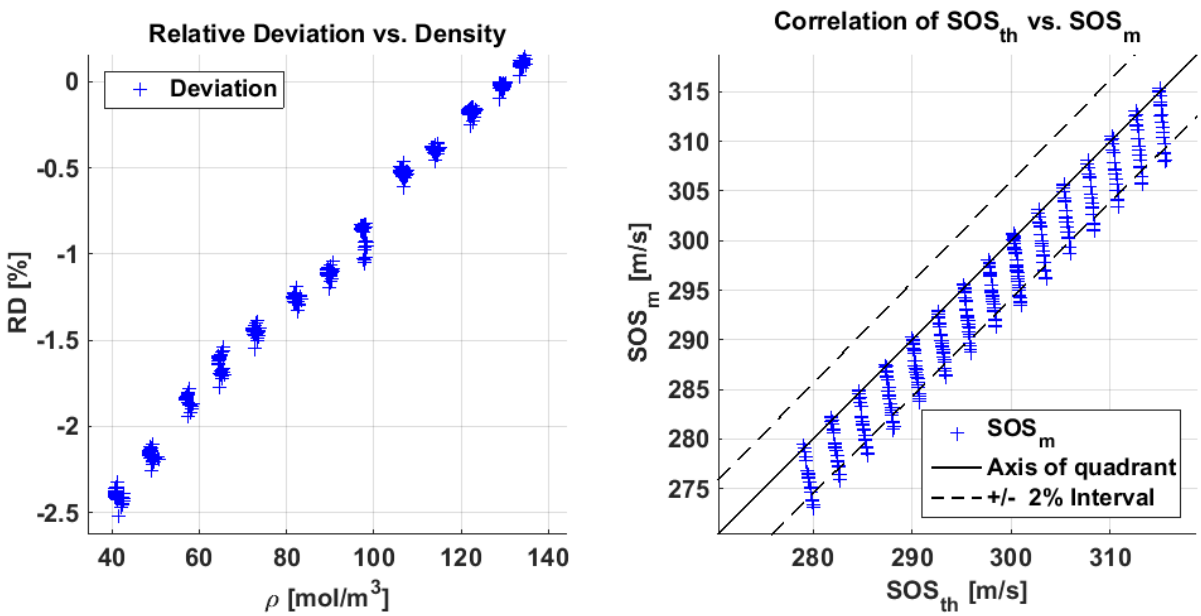

Fig. 21.: Mixture 1. Left: Relative deviation vs. density. Right: Correlation of theory and measurement. The 2% interval is marked for better comparison.

approach the ideal gas behaviour. Possibly, the error originates from what was observed earlier, that PR EOS is less accurate for compounds with low molar mass (like N_2) and becomes accurate for heavier compounds, as C_3F_8. Equally, the error may originate in the measurement setup, which can be pressure sensitive.

The overall correlation is visualised on the bottom right plot, which also shows ± 2% interval for better visualisation. For the most part, the measurement lies within this ± 2% interval (Fig. 21).

9.4 Mixture 2 (6% N_2 and 94% C_3F_8)

Among the acquired datasets, it is the mixture 2 (mostly C_3F_8), which shows the best correlation between the theory and experiment, staying within 2% of each other (Fig. 22). One dataset of this series (ρ=105 mol/m³) was lost due to malfunctioning of electronics.

Deviation rises linearly with density from 0% up to 1.5%. There is a distortion effect with unclear origin appearing approximately in the middle of dataset. It is clearly visible in the relative deviation plot (Fig. 23, left).

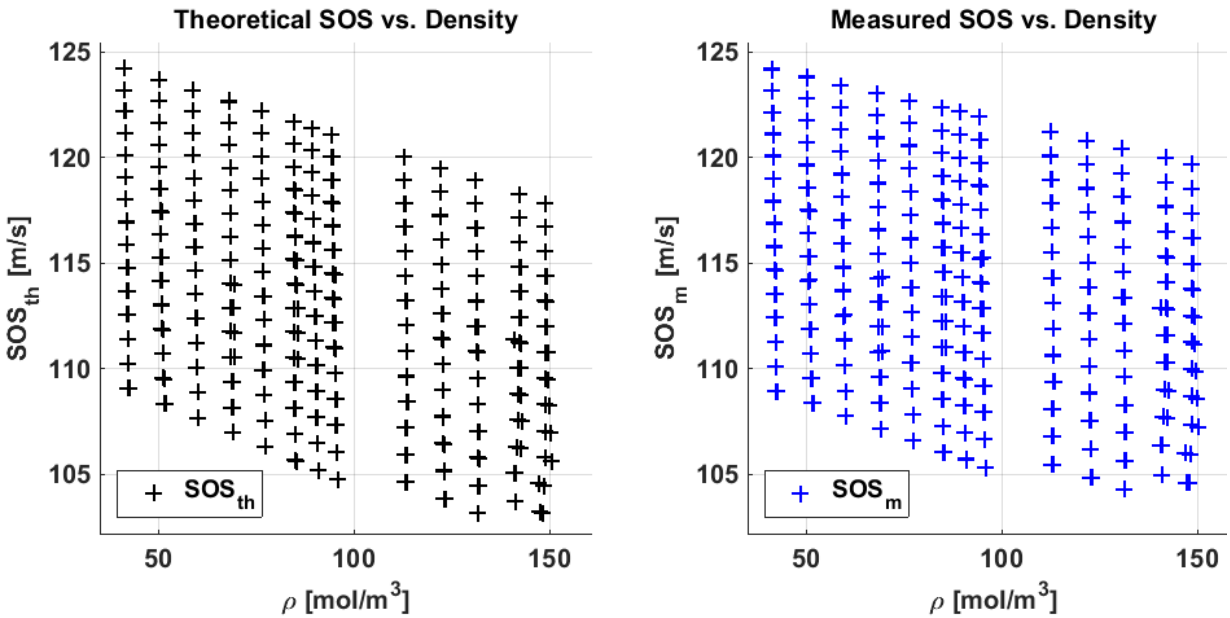

Fig. 22.: Mixture 2 (6% N_2 and 94% C_3F_8). Left: Model prediction. Right: Measured data.

Besides that, data points measured at higher densities exhibit higher variance, i.e. the clusters formed by the points are less compact than at lower densities. It is analysed in the following paragraph, where this tendency is more apparent. To conclude, the overall correlation (Fig. 23, right) lies within 2% interval.

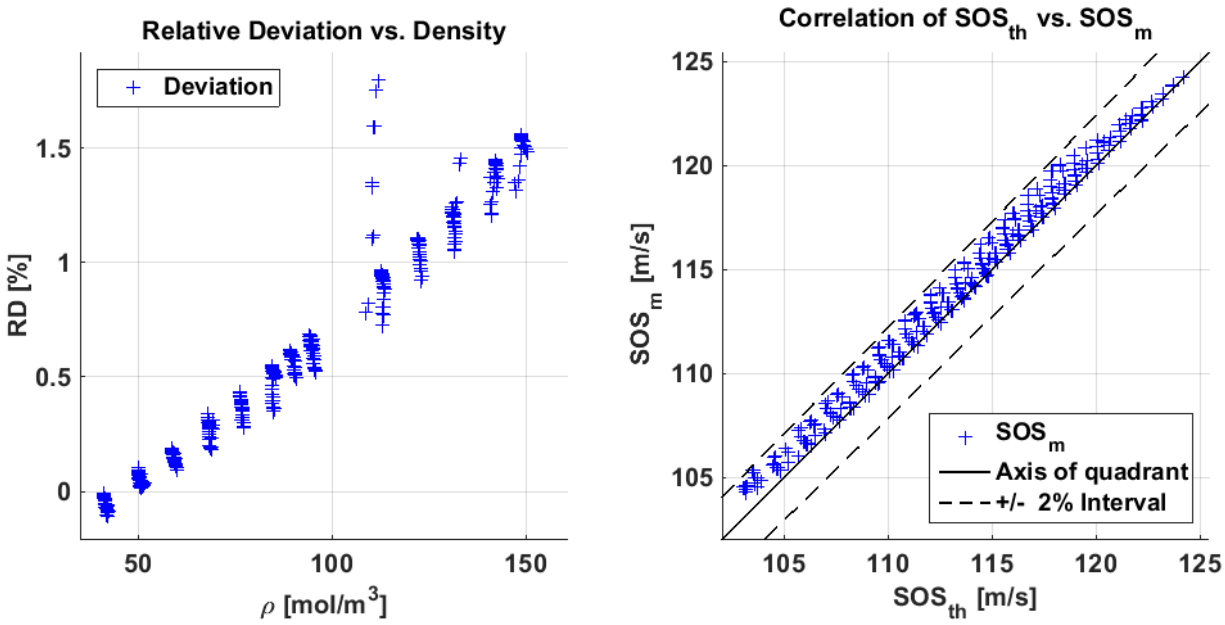

Fig. 23.: Mixture 2. Left: Relative deviation vs. density. Right: Correlation of theory and measurement. The 2% interval is marked for better comparison.

9.5 Mixture 3 (16% N_2 and 84% C_3F_8)

Mixture 3 (rich in C_3F_8) exhibits high accuracy, similar to previous mixture 2. The data is very much alike, except for the distortion at two highest densities (130 and 140 mol/m³). This is probably due to insufficient stabilisation of the system,

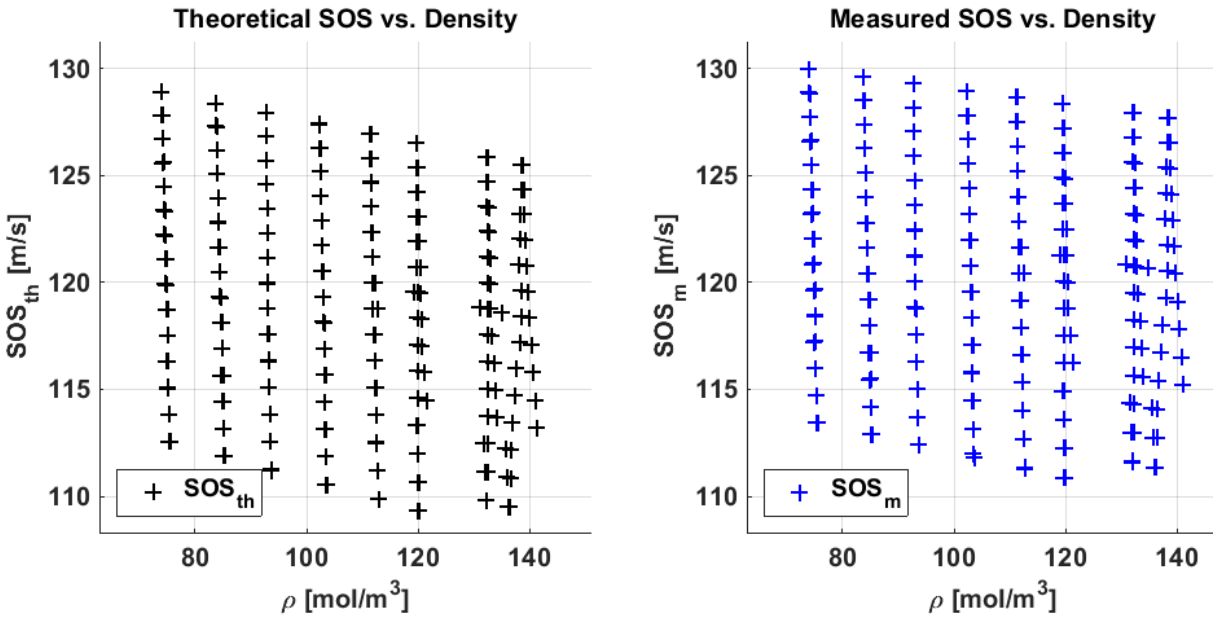

Fig. 24.: Mixture 3 (16% N_2 and 84% C_3F_8). Left: Model prediction. Right: Measured data.

so the thermodynamic equilibrium was not approached enough before taking the measurement. It is also possible that the chiller's performance was compromised by changes in ambient temperature. Despite of this distortion, the measured data seem to be in good concordance with the rest of the dataset and the analytical model and even exhibit somewhat smaller deviation than previous mixtures.

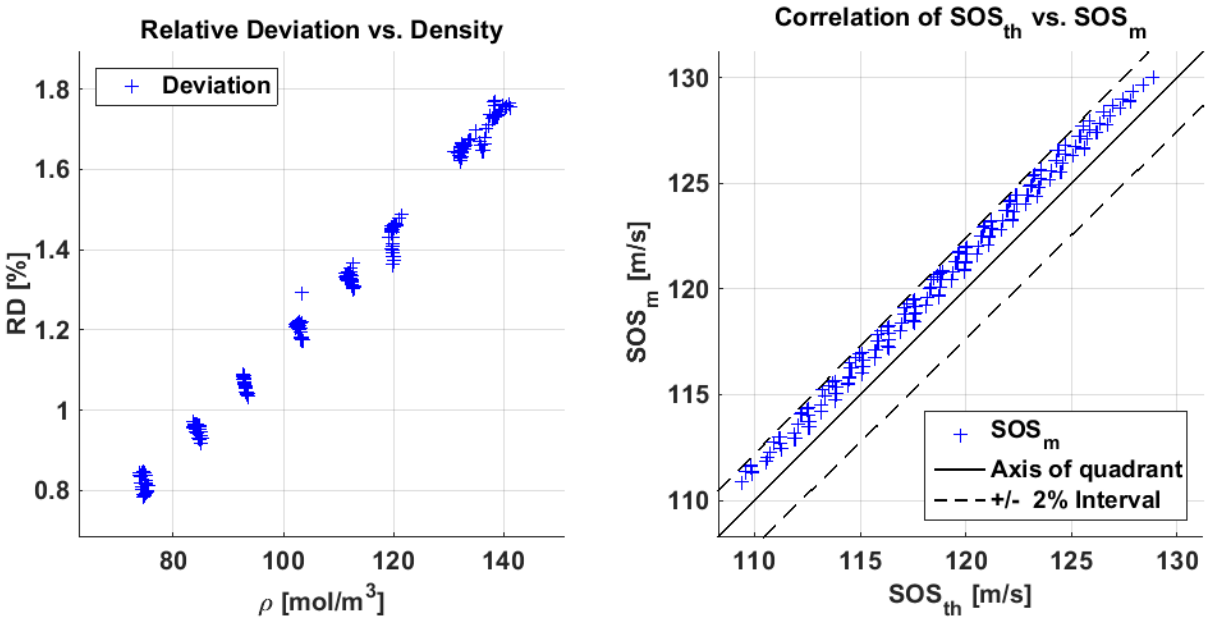

Fig. 25.: Mixture 3. Left: Relative deviation vs. density. Right: Correlation of theory and measurement. The 2% interval is marked for better comparison.

9.6 Summary of experimental investigation

For the great part of the investigated mixtures, the theoretical prediction lies within 2% of the measured values, so the developed scheme (combination: PR EOS, mixing rules, NIST properties) is a reasonably precise estimation technique for the speed of sound calculation. However, this scheme might not be accurate enough for certain applications. For example, the inverse task of determining the composition from a measured SOS would require further improvements to enhance the accuracy of this theoretical model.

Moreover, the linear behaviour of deviation, which persists in all 3 mixtures, should be further examined, because it represents the main source of error. Once this linear behaviour of deviation is removed (Fig. 26), the remaining variance between the theory and experiment decreases by an order of magnitude. This is due to fact, that the clusters of measured points are relatively compact and small in comparison with the linear behaviour of the error. This fact poses a relatively easy mean of enhancing the predictive ability of the theory, simply by subtracting a linear regression from the measured data.

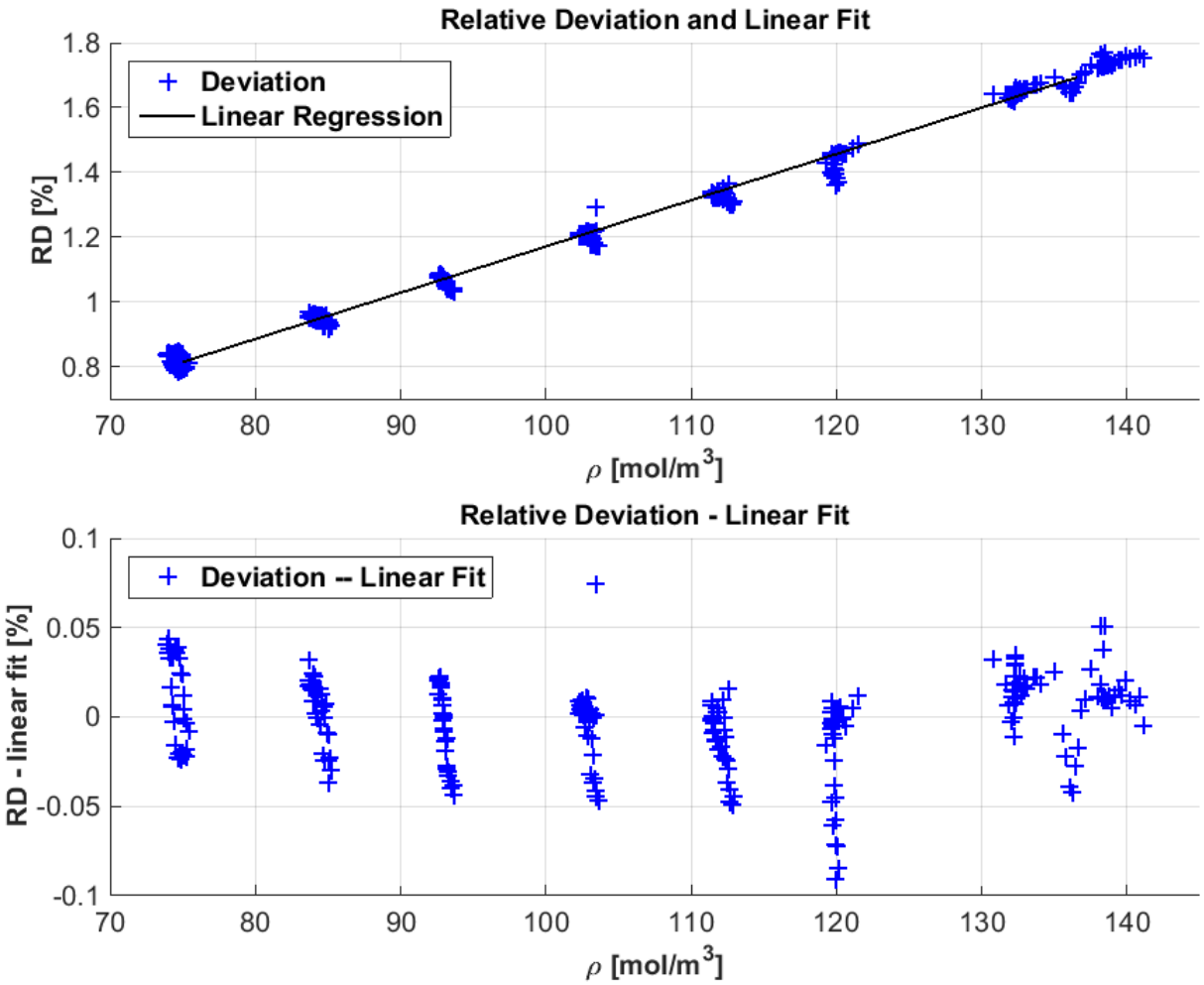

Fig. 26.: Relative Deviation. Linear fit of the deviation was subtracted from it. The remaining variance is by one order smaller than before the linear fit subtraction.

10 Summary and conclusions

10.1 Findings of the theoretical part

The thesis begins with a review of basic concepts of thermodynamics. These concepts were then used in evaluating equations of state and in calculating the speed of sound in mixtures of gases. It was found, that the accurate prediction of speed of sound in a gas of a known composition depends greatly on the accuracy of thermodynamic properties employed in the calculation as well as on accuracy of a state equation, whose derivatives are used.

Multiple descriptions of gas behaviour were outlined, including ideal and real gas concepts. Dealing with real gases requires advanced multi-parameter equations of state, so some of the classical state equations were presented, such as those of Redlich-Kwong and Peng-Robinson. Accuracy of these equations was examined concluding, that the Peng-Robinson state equation is the appropriate choice, while dealing with heavy compounds, like perfluorocarbons. The derivatives of this equation of state were evaluated, as they were needed to determine the residual heat capacity of gases and in the speed of sound calculation.

Different sources of thermodynamic properties were presented. Two group contribution methods were used to calculate properties (critical point, heat capacity) of refrigerants C_2F_6 and C_3F_8 (R-116 and R-218) and their results were confronted with NIST REFPROP thermodynamic properties database. This database is a result of precise measurements and is used as a reference. The Joback-Reid and Constantinou-Gani group contribution methods were tested on the two perfluorocarbon compounds to get an insight into precision of the contribution methods for fluorocarbons. The methods show relative deviation from NIST values of 10% and 2%, respectively. Nonetheless, to get the most accurate results, the NIST properties were used in further calculations.

These compounds' properties were then combined using proper mixing rules, resulting into the Peng-Robinson parameters of a mixture of gases. Because the Peng-Robinson equation has a temperature dependent parameter, it needed to be derived as well, along with its mixing rule.

As a result of the analytical part of the thesis, the speed of sound in a mixture of real gases was calculated, using the combination of Peng-Robinson equation, NIST thermodynamic properties and proper mixing rules.

10.2 Results of the measurement

The motivation for the previous calculation was to have a universally applicable theoretical model, which proficiently describes the speed of sound in a mixture of gases. In our case, the measurement was performed on a binary mixtures of N_2 and C_3F_8, with composition varying from 6 % to 95 % of N_2 in C_3F_8. The choice of mixtures was motivated by direct application to ultrasonic sensors used

in evaporative cooling circuits that employ these fluorocarbons as a cooling liquid. These measurements represent the case when cooling circuit is contaminated with atmospheric air (consisting mostly of N_2).

The whole procedure of measurement and data acquisition was thoroughly described. Possible sources of error in the measurements were discussed and taken into account while processing the measured data. The same evaluation procedure was used for all data sets and mixtures. Data points where condensation occurred were removed before further processing. Then, only histogram peaks with significance greater than 10% were selected for each setpoint, while the rest was neglected in statistical evaluation. When the measured data was evaluated, it could be compared to the analytically calculated values of speed of sound.

Finally, the correlation between the theoretical prediction and results of measurement was examined. For the most part of the collected data points the relative deviation is less than 2 % in terms of the speed of sound at given concentration, temperature and pressure. Generally, this can be considered as a good result, having in mind the relative simplicity of used mathematical description.

10.3 My own contribution

As an outcome of this work, there is a rigorous theoretical basis of the speed of sound calculation using the Peng-Robinson state equation. The whole calculation was performed in MATLAB environment in a form, which enables further use of the developed software.

The code is universally applicable to any mixture of gases, given its chemical composition in terms of molar fractions. It is partitioned into multiple functions. One evaluates thermodynamic properties from group contribution methods (or recalls data from NIST), once the chemical formula is provided. Next function evaluates properties of a mixture and parameters of the Peng-Robinson state equation. Finally, the speed of sound in a mixture is calculated from the state equation derivatives. These derivatives are also essential in determining other thermodynamic properties, such as residual heat capacity, Joule-Thomson coefficient and others, which adds extra potential to the developed program.

10.4 Conclusion

The thesis has met the guidelines and fulfilled the tasks in terms of elaborating a research, calculating analytically the speed of sound in a mixture of real gases and implementing this solution in MATLAB environment. It was found out that the analytical and experimental values of speed of sound in mixtures of N_2 and C_3F_8 differ by 2% from each other in the pressure range of 0.09 – 0.35 MPa and temperature range of 253 - 323 K.

10.5 Suggestion for further study

Further measurements could focus on ternary mixtures of refrigerants and N_2. Possibly, mixtures of refrigerants with O_2 could be measured, as it is the second most abundant gas in the atmosphere. Various sources of error present in the measurements should be investigated and their origin should be determined in order to avoid it in the upcoming measurements. Considering data processing, the interaction coefficients between N_2 and C_3F_8 could be determined from the measured data, as well as part of the saturation curve, since it was reached multiple times during the measurement of C_3F_8-rich mixtures.

At last, some more advanced state equations, based on simulation methods will be of interest. For example, some type of statistical associating fluid theory (SAFT) equation of state can be used to simulate the behaviour of gas mixtures.

11 Bibliography

[1] NOŽIČKA, J. Základy termomechaniky. Vyd. 1. Praha: Vydavatelství ČVUT, 2001, 187 s. ISBN 80-01-02409-1.

[2] NOVÁK, Josef. Termodynamické vlastnosti plynů. Vyd. 1. Praha: Vydavatelství VŠCHT Praha, 2007, xiv, 222 s. ISBN 978-80-7080-630-2.

[3] PENG, Ding-Yu and Donald B. ROBINSON. A New Two-Constant Equation of State. Industrial & Engineering Chemistry Fundamentals [online]. 1976, vol. 15, issue 1, s. 59-64 [cit. 2015-05-04]. DOI: 10.1021/i160057a011.

[4] PEDERSEN, K. and P. L. CHRISTENSEN. Phase behavior of petroleum reservoir fluids. Boca Raton: CRC/Taylor & Francis, c2007, 406 p. ISBN 9780824706944.

[5] IUPAC. Compendium of Chemical Terminology, 2nd ed. (the "Gold Book"). Compiled by A. D. McNaught and A. Wilkinson. Blackwell Scientific Publications, Oxford (1997). XML on-line corrected version: http://goldbook.iupac.org (2006) created by M. Nic, J. Jirat, B. Kosata; updates compiled by A. Jenkins. ISBN 0-9678550-9-8. DOI: 10.1351/goldbook.

[6] National Institute of Standards and Technology (NIST), Standard reference database. REFerence fluid PROPerties (REFPROP). Version 9.0 [software]. 2010.

[7] KWAK, T. Y., MANSOORI, G. A. Van der Waals mixing rules for cubic equations of state, Applications for supercritical fluid extraction modelling. Chemical Engineering Science, Vol. 41, No. 5, pp. 1303-1309. 1986.

[8] KOLSKÁ, Z.; ZÁBRANSKÝ, M.; RANDOVÁ, A.: Group contribution methods for estimation of selected physico-chemical properties of organic compounds. In: Thermodynamics - Fundamentals and Its Application in Science. (Ed. Ricardo Morales-Rodriguez), In Tech d.o.o., Rijeka, Croatia, 136-162 (2012). ISBN 978-953-51-0779-8.

[9] POLING, B. E, J PRAUSNITZ and J. P O'CONNELL. The properties of gases and liquids. 5th ed. New York: McGraw-Hill, c2001, 1 v. ISBN 0070116822-.

[10] MARRERO, J. and R. GANI. Group-contribution based estimation of pure component properties. Fluid Phase Equilibria [online]. 2001, 183-184, s. 183-208 [cit.2015-05-02]. DOI: 10.1016/s0378-3812(01)00431-9.

[11] PRATT, R.M. Thermodynamic Properties Involving Derivatives Using the Peng-Robinson Equation of State. J. Chem. Eng. Ed. Vol. 35, No. 2 pp. 112-115, 2001. On-line version: http://ufdc.ufl.edu/AA00000383/00150

[12] CHUEH, P. L. a J. M. PRAUSNITZ. Vapor-liquid equilibria at high pressures: Calculation of partial molar volumes in nonpolar liquid mixtures. AIChE Journal [online]. 1967, 13(6): 1099-1107 [cit. 2015-06-12]. DOI: 10.1002/aic.690130612.

[13] DOUBEK, M. *Studie zařízení pro měření rychlosti zvuku v plynné fázi.* Praha: CTU Prague, 2012. Bachelor thesis, CTU Prague, Faculty of Mechanical Engineering, Department of Fluid Dynamics and Thermodynamics.

[14] DOUBEK, M. *Thermophysical properties of fluids, experiment and simulations.* Praha: CTU Prague, 2014. Master thesis, CTU Prague, Faculty of Mechanical Engineering, Department of Fluid Dynamics and Thermodynamics.

[15] YAWS, C.L. Thermophysical properties of chemicals and hydrocarbons. Second edition. viii, 991 pages. ISBN 9780323286596.

[16] RIAZI, M.R. and MANSOORI, G.A., "An Accurate Equation of State for Hydrocarbon Systems," Presented at 1993 AIChE Spring National Meeting, Houston, Texas, USA (March 28 - April 1, 1993).

[17] VACEK, V., G. HALLEWELL and S. LINDSAY. Velocity of sound measurements in gaseous per-fluorocarbons and their mixtures. Fluid Phase Equilibria [online]. 2001, vol. 185, 1-2, s. 305-314 [cit. 2015-05-04]. DOI: 10.1016/s0378-3812(01)00479-4.

[18] VACEK, Václav, Michal VÍTEK a Martin DOUBEK. Velocity of sound in Perfluoropropane (C3F8), Perfluoroethane (C2F6) and their mixtures. Fluid Phase Equilibria [online]. 2013, 351: 53-60 [cit. 2015-06-12]. DOI: 10.1016/j.fluid.2012.10.002.

[19] BATES, Richard, Michele BATTISTIN, Stephane BERRY, Alexander BITADZE, Pierre BONNEAU, Nicolas BOUSSON, George BOYD, Gennaro BOZZA, Olivier CRESPO-LOPEZ, et al. Implementation of Ultrasonic Sensing for High Resolution Measurement of Binary Gas Mixture Fractions. Sensors [online]. 2014, 14(6): 11260-11276 [cit. 2015-06-12]. DOI: 10.3390/s140611260.

[20] YUNUS A. CENGEL, Yunus A.Michael A. Thermodynamics: an engineering approach. 4th ed. Boston, [Mass.]: McGraw-Hill, 2002. ISBN 007121688x.

[21] SPAN, R., E. W. LEMMON, R. T. JACOBSEN, W. WAGNER, and A. YOKOZEKI. A Reference Equation of State for the Thermodynamic Properties of Nitrogen for Temperatures from 63.151 to 1000 K and Pressures to 2200 MPa. Journal of Physical and Chemical Reference Data [online]. 2000, 29(6) [cit. 2015-06-12]. DOI: 10.1063/1.1349047.

[22] JAUBERT, Jean-Noël a Fabrice MUTELET. VLE predictions with the Peng-Robinson equation of state and temperature dependent kij calculated through a group contribution method. Fluid Phase Equilibria [online]. 2004, 224(2): 285-304 [cit. 2015-06-12]. DOI: 10.1016/j.fluid.2004.06.059.

12 List of figures

Figure	1.	Phase diagram (simplified)	2
Figure	2.	Acentric factor. Modified from: Wikimedia Commons. Accessible on-line: http://commons.wikimedia.org/wiki/File%3AOctafluoropropane_3D_ball.png	3
Figure	3.	Sound wave propagation	6
Figure	4.	Generalized compressibility chart. [20]	9
Figure	5.	Schematic p-V diagram of a real gas	10
Figure	6.	Accuracy of RK and PR EOS	14
Figure	7.	Mixing rules	16
Figure	8.	Group decomposition	20
Figure	9.	Structure of MATLAB code 1	24
Figure	10.	Structure of MATLAB code 2	25
Figure	11.	Speed of sound in a mixture vs. Composition and Temperature	25
Figure	12.	Scheme of transition time measurement	26
Figure	13.	Scheme of the measurement hardware	27
Figure	14.	SensComp 600 ultrasonic capacitive transducer. SensComp Inc. "Series 600 Ultrasonic Sensors." Electrostatic Ultrasonic Sensors. 2012 SensComp Inc., n.d. Web. 14 May 2015. http://www.senscomp.com/ultrasonic-sensors	27
Figure	15.	Scheme of electronics and instrumentation	28
Figure	16.	Graphical user interface of WinCC OA	30
Figure	17.	Measurement of one mixture at different pressures	31
Figure	18.	Selecting data points using histogram	32
Figure	19.	Condensation occurrence during measurement	33
Figure	20.	Mixture 1.: Model vs. measurement	34
Figure	21.	Mixture 1.: Deviation and correlation	34
Figure	22.	Mixture 2.: Model vs. measurement	35
Figure	23.	Mixture 2.: Deviation and correlation	36
Figure	24.	Mixture 3.: Model vs. measurement	36
Figure	25.	Mixture 3.: Deviation and correlation	37
Figure	26.	Investigation of relative deviation	38

13 List of tables

Table 1. Acentric factor 3

Table 2. Redlich-Kwong and Peng-Robinson equation of state accuracy 13

Table 3. Coefficients of Joback and Reid 21

Table 4. Coefficients of Constantinou and Gani 22

Table 5. Accuracy of JR and CG methods compared to NIST REFPROP 23

Table 6. Measured mixtures of N_2 and C_3F_8 33

14 Appendix A – Developed MATLAB code

COEFFICIENTS.xls

Joback and Reid coefficients [9]

	Tb	Tc	Pc	Vc	A	B	C	D	M
	[K]	[K]	[bar]	[cm^3/mol]			[J/K.mol]		[g/mol]
C	18.25	0.0067	0.0043	27.00	-66.20	0.4270	-6.41E-04	3.01E-07	12.01
F	-0.03	0.0111	-0.0057	27.00	26.50	-0.0913	1.91E-04	-1.03E-07	19.00
Cl	38.13	0.0105	-0.0049	58.00	33.30	-0.0963	1.87E-04	9.96E-08	35.45
CH	21.74	0.0164	0.0020	41.00	-23.00	0.2040	-2.65E-04	1.20E-07	13.02
CH_2	22.88	0.0189	0.0000	56.00	-0.91	0.0950	-5.44E-05	1.19E-08	14.03
CH_3	23.58	0.0141	-0.0012	65.00	19.50	-0.0081	1.53E-04	-9.67E-08	15.03

Constantinou and Gani coefficients [9]

	Tb	Tc	Pc	Vc	A	B	C	D	M
	[K]	[K]	[bar]	[m^3/kmol]			[J/K.mol]		[g/mol]
CF_3	1.2880	2.4778	0.0442	0.1148	63.2024	51.9366	-28.6308	0	69.0059
CF_2	0.6115	1.7399	0.0129	0.0952	44.3567	44.5875	-23.282	0	50.0075
CF	1.1739	3.5192	0.0047	-	-	-	-	-	31.0091
CCl_2F	2.8881	9.8408	0.0354	0.1821	-	-	-	-	101.9151
$CClF_2$	1.9163	4.8923	0.0390	0.1475	-	-	-	-	85.4605
C	0.2878	4.8823	-0.0104	-0.0003	0.3456	74.0368	-45.7878	0	12.0107
CH	0.6033	4.0330	0.0013	0.0315	8.9272	59.9786	-29.5143	0	13.0186
CH_2	0.9225	3.4920	0.0106	0.0558	22.6346	45.0933	-15.7033	0	14.0266
CH_3	0.8894	1.6781	0.0199	0.0750	35.1152	39.5923	-9.9232	0	15.0345

NIST REFPROP database values [6]

	A	B	C	D	M	Tb	Tc	Pc	Vc	ω
	[J/K.mol]				[g/mol]	[K]	[K]	[MPa]	[m^3/mol]	[-]
N_2	1.9494E-08	-1.2581E-05	2.7756E-03	28.90000	28.013	77.3550	126.1900	3.3958	8.9413E-05	0.0372
C_2F_6	-6.5213E-08	-2.1480E-04	3.6319E-01	18.95000	138.010	195.0600	293.0300	3.0480	2.2502E-04	0.2566
C_3F_8	5.2206E-07	-8.1079E-04	6.4085E-01	15.15400	188.020	236.3600	345.0200	2.6400	2.9940E-04	0.3172
O_2	3.1522E-08	-1.6200E-06	-2.6104E-03	29.46200	31.999	90.1880	154.5800	5.0430	7.3368E-05	0.0222
CO_2	-2.2721E-07	1.5298E-04	1.5376E-02	24.98200	44.010	-	304.1300	7.3773	9.4118E-05	0.2239
Ar	0	0	0	20.78628	39.948	87.3020	150.6900	4.8630	7.4588E-05	-0.0022
Xe	0	0	0	20.78618	131.290	165.0500	289.7300	5.8420	1.1905E-04	0.0036
Air	2.1810E-08	-1.0143E-05	1.6133E-03	28.94400	28.966	7842030	132.5306	3.7860	8.4525E-05	0.0335

JR.m

```
function [PROPS] = JR(compound)
%% Joback-Reid method:
% Input:  string: 'C2F6' or 'C3F8' or 'N2'
% Output: vector of compounds' properties
%  [D C B A  M     Tb Tc Pc Vc     RhoC  w]
%   J/K.mol  g/mol K  K  Pa m3/mol kg/m3 1]

%% Group decomposition of chosen compound
switch compound
    case 'C3F8'
        Groups_JR_Count=[3 8 0 0 0 0 ]';
        w=0.317;    % Acentric factor

    case 'C2F6'
        Groups_JR_Count=[2 6 0 0 0 0 ]';
        w=0.257;    % Acentric factor

    case 'N2'       % Foolproof: N2 from NIST
        PROPS=xlsread('COEFS.xls','NIST','B1:L1')';
        fprintf('JR called  NIST \n')
        PROPS(8)=1e6*PROPS(8);       % [MPa->Pa]
        return
end
%% Read Coefs from JR tabless
Coefs_JR=xlsread('COEFFICIENTS.xls','JR');

%% Ideal Isobaric Heat Capacity Cp0
% Polynomial Coefs      [J/K.mol]
A=sum(Groups_JR_Count.*Coefs_JR(:,5))-37.93;
B=sum(Groups_JR_Count.*Coefs_JR(:,6))+0.21;
C=sum(Groups_JR_Count.*Coefs_JR(:,7))-3.91e-4;
D=sum(Groups_JR_Count.*Coefs_JR(:,8))+2.06e-7;
%% Molar mass            [g/mol]
M=sum(Groups_JR_Count.*Coefs_JR(:,9));
Na=sum(Groups_JR_Count);
%% Boiling point         [K]
Tb_sum=sum(Groups_JR_Count.*Coefs_JR(:,1));
Tb=198+Tb_sum;
%% Critical Temperature  [K]
Tc_sum=sum(Groups_JR_Count.*Coefs_JR(:,2));
Tc=Tb*(0.584+0.965*Tc_sum-Tc_sum^2)^-1;
%% Critical Pressure     [MPa]
Pc_sum=sum(Groups_JR_Count.*Coefs_JR(:,3));
Pc=(0.113+0.0032*Na-Pc_sum)^-2;      % [bar]
Pc=0.1*Pc;                           % [MPa]
Pc=1e6*Pc;                           % [Pa]
%% Critical Volume       [m3/mol]
Vc_sum=sum(Groups_JR_Count.*Coefs_JR(:,4));
Vc=(17.5+Vc_sum)*10^-6;
%% Critical Density      [kg/m3]
RhoC=10^-3*M/Vc;
%% Output
PROPS=[D C B A M Tb Tc Pc Vc RhoC w]';
return
end
```

CG.m

```
function [PROPS] = CG(compound)
%% Constantinou-Gani method: 1st order only(W=0)
% Input:  string: 'C2F6' or 'C3F8' or 'N2'
% Output: vector of compounds' properties
%  [D C B A  M     Tb Tc Pc Vc     RhoC  w]
%   J/K.mol  g/mol K  K  Pa m3/mol kg/m3 1]

%% Group decomposition of chosen compound
switch compound
    case 'C3F8'
        Groups_CG_Count=[2 1 0 0 0 0 0 0 0]';
        w=0.317;    % Acentric factor

    case 'C2F6'
        Groups_CG_Count=[2 0 0 0 0 0 0 0 0]';
        w=0.257;    % Acentric factor

    case 'N2'       % Foolproof: N2 from NIST
        PROPS=NIST('N2');
        fprintf('CG called  NIST\n')
        return
end

%% Read Coefs from CG tables
Coefs_CG=xlsread('COEFFICIENTS.xls','CG');

%% Ideal Isobaric Heat Capacity Cp0
% Polynomial Coefs      [J/K.mol]
A=sum(Groups_CG_Count.*Coefs_CG(:,5))-19.7779;
B=sum(Groups_CG_Count.*Coefs_CG(:,6))+22.5981;
C=sum(Groups_CG_Count.*Coefs_CG(:,7))-10.7983; D=0;
% MUST use "pseudo"Temp 'theta' to eval the polynome
%% Molar mass            [g/mol]
M=sum(Groups_CG_Count.*Coefs_CG(:,9));
%% Boiling point         [K]
Tb_sum=sum(Groups_CG_Count.*Coefs_CG(:,1));
Tb=204.359*log(Tb_sum);
%% Critical Temperature  [K]
Tc_sum=sum(Groups_CG_Count.*Coefs_CG(:,2));
Tc=181.128*log(Tc_sum);
%% Critical Pressure     [MPa]
Pc_sum=sum(Groups_CG_Count.*Coefs_CG(:,3));
Pc=(Pc_sum+0.10022)^-2+1.3705;       % [bar]
Pc=0.1*Pc;                           % [MPa]
Pc=1e6*Pc;                           % [Pa]
%% Critical Volume       [m3/mol]
Vc_sum=sum(Groups_CG_Count.*Coefs_CG(:,4));
Vc=(-0.00435 + (Vc_sum))*10^-3;
%% Critical Density      [kg/m3]
RhoC=10^-3*M/Vc;
%% Output
PROPS=[D C B A M Tb Tc Pc Vc RhoC w]';
return
end
```

NIST.m

```
function [PROPS] = NIST( compound )
%% NIST properties:
% Input:  string: 'C2F6' or 'C3F8' or N2
% Output: vector of compounds' properties
%  [D C B A  M     Tb Tc Pc  Vc     RhoC  w]
%   J/K.mol  g/mol K  K  MPa m3/mol kg/m3 1]
%
% NIST properties for chosen compound
% as retrieved from NIST REFPROP, saved into COEFS.xls
% Cpo(T) regressed from NIST data for T=(200,330)

switch compound
    case 'N2'
        PROPS=xlsread('COEFFICIENTS.xls','NIST','B1:L1')';
    case 'C2F6'
        PROPS=xlsread('COEFFICIENTS.xls','NIST','B2:L2')';
    case 'C3F8'
        PROPS=xlsread('COEFFICIENTS.xls','NIST','B3:L3')';
    case 'O2'
        PROPS=xlsread('COEFFICIENTS.xls','NIST','B4:L4')';
    case 'CO2'
        PROPS=xlsread('COEFFICIENTS.xls','NIST','B5:L5')';
    case 'AR'
        PROPS=xlsread('COEFFICIENTS.xls','NIST','B6:L6')';
    case 'XE'
        PROPS=xlsread('COEFFICIENTS.xls','NIST','B7:L7')';
    case 'AIR'
        PROPS=xlsread('COEFFICIENTS.xls','NIST','B8:L8')';
end
%% Output
PROPS(8)=1e6*PROPS(8); % Pressure [MPa -> Pa]
return
end
```

PR_params.m

```
function [ A,DA,DDA,B,M,Cp0_MIX ] = PR_params( ID,x,t,METHOD )
% Calculates parameters of PR EoS
% Input:  ID    of mixture components {'N2' 'C2F6'}
%         x     molar fractions of components [0.1 0.9]
%         t     vector of temperatures
% Output: A, DA DDA, B      params(and their derivs) of PR EoS
%         M  [g/mol]        molar mass of mixture
%         Cp0_mix [J/K.mol] ideal isobar heat cap of mix

%% Load Component Properties from NIST/CG/JR
%  (N2 always from NIST)
switch METHOD
    case 'JR'
        for i=1:length(ID)
            Props(i,:)=JR(char(ID(i)));
        end
    case 'CG'
        for i=1:length(ID)
            Props(i,:)=CG(char(ID(i)));
        end
```

```
    case 'NIST'
        for i=1:length(ID)
            Props(i,:)=NIST(char(ID(i)));
        end
end

Props=Props';
w=  Props(11,:);         % Acentric factors
Tc= Props(7,:);          % Temps at Crit. Point
Pc= Props(8,:);          % Press at Crit. Point
Mm= Props(5,:);          % Molar mass
Cp0_Coefs=Props(1:4,:); % Coefs of Heat Capacity
%% PR Consts for Components separately
R=  8.3144621;                   % J/K.mol
b=  0.0077796074*R.*Tc./Pc;
ac= 0.45723553.*(R.*Tc).^2./Pc;
m=polyval([-0.26992  1.54226  0.37464],w);
%% PR Params (and derivs)  a, a', a"  for Components
for k=1:length(t)
    T=t(k);
    for i=1:length(ID)
        alfa(k,i)= (1+m(i)*(1-sqrt(T/Tc(i))))^2;
        a(k,i)= ac(i)*alfa(k,i);
        da(k,i)= -m(i)*a(k,i)/...
            ((1+m(i)*(1-sqrt(T/Tc(i))))*sqrt(T*Tc(i)));
        dda(k,i)= (ac(i)*(m(i)+m(i)^2)*...
            sqrt(Tc(i)/T))/(2*T*Tc(i));
    end
end
%% PR Params (and derivs)  a, a', a"  for MIXTURE
M=   sum(x.*Mm);         % Aparent molar mass
B=   sum(x.*b);          % "b" constant in PR EOS
for k=1:length(t)
    A(k)=  0;
    DA(k)= 0;
    DDA(k)=0;
    for i=1:length(ID)
        for j=1:length(ID)
            A(k)= A(k)+ x(i)*x(j)*sqrt(a(k,i)*a(k,j));
            DA(k)= DA(k)+ x(i)*x(j)*...
                (sqrt(a(k,j)/a(k,i))*da(k,i)+...
                sqrt(a(k,i)/a(k,j))*da(k,j));
            DDA(k)= DDA(k)+  x(i)*x(j)*...
                (((da(k,i)*da(k,j)+dda(k,i)*a(k,j)+...
                a(k,i)*dda(k,j))/sqrt(a(k,i)*a(k,j)))...
                -0.5*((da(k,i)^2*sqrt(a(k,j)/a(k,i)^3))+...
                (da(k,j)^2*sqrt(a(k,i)/a(k,j)^3))));
        end
    end
    DA(k)= DA(k)/2;     % 0.5 * Sum
    DDA(k)=DDA(k)/2;    % 0.5 * Sum
end
% %% Derivativess checked numerically
A=A';
DA=DA';
DDA=DDA';
%% Mixture heat capacity JR/NIST only
Cp0_MixCoefs= (x*Cp0_Coefs')';
Cp0_MIX= polyval(Cp0_MixCoefs,t)';
return
end
```

PR_mix.m

```
function [ SOS, Rho ] = PR_mix( ID,x,t,p,METHOD )
%% ID...composition {'N2' 'C3F8' 'C2F6' 'O2'}
%   x...molar fractions (=partial pressures)
%   t...temperature vector
%   p...pressure vector
%   METHOD...= {'JR/CG/NIST'}

%% Check composition
if (sum(x) ~= 1)            % Molar Fraction SUM = 1
    fprintf('SUM of Molar Fractions = 1 ! \n');
    return
else end

%% LOAD MIXTURE PARAMETERS %%%%%%%%%%%%%%%%%%%%%%%%%%%%%%%%%%%%%%%
[ a da dda b M Cp0 ] = PR_params( ID,x,t,METHOD );
Cp0=Cp0';
R=  8.3144621;              % J/K.mol
%% VOLUME calculation %%%%%%%%%%%%%%%%%%%%%%%%%%%%%%%%%%%%%%%%%%%%%
for i=1:length(t)
    A=a(i);
    T=t(i);
    P=p(i);
    V(i)=real(((R*T - b*P)^3/(27*P^3) +(((R*T - b*P)^3/(27*P^3)-…
        (P*b^3 + R*T*b^2 - A*b)/(2*P) + ((R*T - b*P)*(3*P*b^2 + ...
        2*R*T*b - A))/(6*P^2))^2 - ((R*T - b*P)^2/(9*P^2) + ...
        (3*P*b^2 + 2*R*T*b  A)/(3*P))^3)^(1/2)-(P*b^3 + R*T*b^2 ...
        - A*b)/(2*P) + ((R*T - b*P)*(3*P*b^2 + 2*R*T*b - A))/...
        (6*P^2))^(1/3) + (R*T-b*P)/(3*P)+((R*T - b*P)^2/(9*P^2) ...
        + (3*P*b^2 + 2*R*T*b - A)/(3*P))/((R*T - b*P)^3/(27*P^3)+...
        (((R*T - b*P)^3/(27*P^3) - (P*b^3 + R*T*b^2 - A*b)/(2*P)+...
        ((R*T - b*P)*(3*P*b^2 + 2*R*T*b - A))/(6*P^2))^2 - ...
        ((R*T - b*P)^2/(9*P^2) +(3*P*b^2 + 2*R*T*b - A)/...
        (3*P))^3)^(1/2) - (P*b^3 + R*T*b^2 - A*b)/(2*P) + ...
        ((R*T - b*P)*(3*P*b^2 + 2*R*T*b - A))/(6*P^2))^(1/3));
end
Rho=1./V;
V=V';

%% Compressibility Factor
Z=P*V/(R*T);
B=b*P/(R*T);
%% DERIVATIVES of PR EOS
dPdV = (-R.*t)./((V-b).^2)+(2.*a.*(V+b))./((V.^2+2*b.*V-b^2).^2);
dPdT = (R)./(V-b)-(da)./(V.^2+2*b.*V-b^2);
dTdP = 1./dPdT;
dVdT = -dPdT./dPdV; % Cycl. deriv. rule: dPdV.*dTdP.*dVdT=-1
%% HEAT CAPACITIES
Cv0=Cp0-R;
CvR=(t.*dda./((sqrt(8)*b))).*log((Z+B.*...
    (1+sqrt(2)))./(Z+B.*(1-sqrt(2))));
Cv=Cv0+CvR;                                 % Isochor. capacity
CpR=t.*dPdT.*dVdT-R+CvR;
Cp=Cp0+CpR;                                 % Isobar.  capacity
%% POISSON RATIO
kappa=(Cp./Cv);
%% SOS
SOS=V.*sqrt(-kappa.*dPdV./(0.001*M));
end
```

SOS.m

```
clear all; clc; close all;
format compact; format shorteng;

%% INPUT COMPOSITION & METHOD  %%%%%%%%%%%%%%%%%%%%%%%%%%%%%%%%%%%%
ID=    {'N2' 'C3F8'};    % Composition N2/C2F6/C3F8/O2/CO2/AR/XE
METHOD= 'NIST';          % Method JR/NIST

for i=1:3
    switch i
        case 1
            file='ResMix6.xls';
            x=  [ 0.954 0.046];      % Molar Fraction
        case 2
            file='ResMix7.xls';
            x=  [ 0.063 0.937];      % Molar Fraction
        case 3
            file='ResMix8.xls';
            x=  [ 0.157 0.843];      % Molar Fraction
    end

    %% SOS MEASUREMENT      %%%%%%%%%%%%%%%%%%%%%%%%%%%%%%%%%%%%%%%%
    G=  importdata(file);          % Import pre-processed data
    P=  G.data(:,1)*1e5;           % Conversion: bar->Pa
    T=  G.data(:,3)+273.15;        % Conversion: °C->K
    SOSmeasure= G.data(:,5);

    %% SOS THEORY   %%%%%%%%%%%%%%%%%%%%%%%%%%%%%%%%%%%%%%%%%%%%%%%%%
    [SOStheory Rho]=PR_mix( ID,x,T,P,METHOD );
    % Relative deviation
    RD= 100*(SOSmeasure-SOStheory)./SOStheory;

    %%%%%%%%%%%%%%%%%%%%%%%%%%%%%%%%%%%%%%%%%%%%%%%%%%%%%%%%%%%%%%%%
    %% GRAPHICS
    % Format
    line= 1.14;
    font= 15;
    size= 9;
    interval= 1.02;
    front= 0.85;
    back= 1.07;
    SOSmin= .99*min(min([SOStheory,SOSmeasure]));
    SOSmax= 1.01*max(max([SOStheory,SOSmeasure]));
    RHOmin= front*min(Rho);
    RHOmax= back*max(Rho);
    RDmin=  min(RD)-0.1;
    RDmax=  back*max(RD);
    a=0.38; b=0.48;
    %% GRAF1
    figure(2*i-1);
    set(gcf,'units','normalized','outerposition',[a b 1-a 1-b]);
    % sub1
    subplot(1,2,1); hold on; grid on;
    plot(Rho,SOStheory,'k+','LineWidth',line, 'MarkerSize',size);
    set(gca,'fontsize',font,'FontWeight','bold');
    axis([RHOmin RHOmax SOSmin SOSmax]); axis square;
    xlabel( '\rho [mol/m^3]','FontSize',font,'FontWeight','bold');
    ylabel( 'SOS_{th} [m/s]','FontSize',font,'FontWeight','bold');
    title('Theoretical SOS vs. Density','FontSize',...
```

```
        font,'FontWeight','bold')
    legend({'SOS_{th}'},'Location','southwest',...
        'FontSize',font-1,'FontWeight','bold')
    % sub2
    subplot(1,2,2); hold on; grid on;
    plot(Rho,SOSmeasure,'b+','LineWidth',line, 'MarkerSize',size);
    set(gca,'fontsize',font,'FontWeight','bold');
    axis([RHOmin RHOmax SOSmin SOSmax]);
    xlabel( '\rho [mol/m^3]','FontSize',font,'FontWeight','bold');
    ylabel( 'SOS_{m} [m/s]','FontSize',font,'FontWeight','bold');
    title('Measured SOS vs. Density','FontSize',font,'FontWeight','bold');
    legend({'SOS_{m}'},'Location','southwest','FontSize',...
        font-1,'FontWeight','bold');
    axis square;
    %% GRAF2
    figure(2*i);
    set(gcf,'units','normalized','outerposition',[a b 1-a 1-b]);
    % sub1
    subplot(1,2,1); hold on; grid on;
    plot(Rho,RD,'b+','LineWidth',line-0.018, 'MarkerSize',size-1);
    set(gca,'fontsize',font,'FontWeight','bold');
    axis([RHOmin RHOmax RDmin RDmax]);
    xlabel( '\rho [mol/m^3]','FontSize',font,'FontWeight','bold');
    ylabel( 'RD [%]','FontSize',font,'FontWeight','bold');
    title(  'Relative Deviation vs. Density','FontSize',...
        font,'FontWeight','bold');
    legend({'Deviation'},'Location','northwest',...
        'FontSize',font-1,'FontWeight','bold');
    axis square;
    % sub2
    subplot(1,2,2); hold on; grid on;
    plot(SOStheory,SOSmeasure,'b+','LineWidth',...
        line-0.018,'MarkerSize',size-1);
    set(gca,'fontsize',font,'FontWeight','bold');
    plot([0 SOSmax],[0 SOSmax],'k-','LineWidth',1.5,'MarkerSize',size+1);
    plot([0 SOSmax],[0 interval*SOSmax],'k--','LineWidth',1.25,...
        'MarkerSize',size+1);
    plot([0 interval*SOSmax],[0 SOSmax],'k--','LineWidth',1.25,...
        'MarkerSize',size+1);
    axis([SOSmin SOSmax SOSmin SOSmax]);
    axis square;
    xlabel( 'SOS_{th} [m/s]','FontSize',font,'FontWeight','bold');
    ylabel( 'SOS_{m} [m/s]','FontSize',font,'FontWeight','bold');
    title(  'Correlation of SOS_{th} vs. SOS_{m}','FontSize',...
        font,'FontWeight','bold');
    legend({'SOS_{m}','Axis of quadrant','+/-  2% Interval'},...
        'Location','southeast','FontSize',font-1);
end
```

15 Appendix B – Enclosed CD

The enclosed CD contains electronic version of this work in *.docx* and *.pdf* formats, measured and processsed data are stored in *.xls* sheets and developed MATLAB code is published in *.m* files.